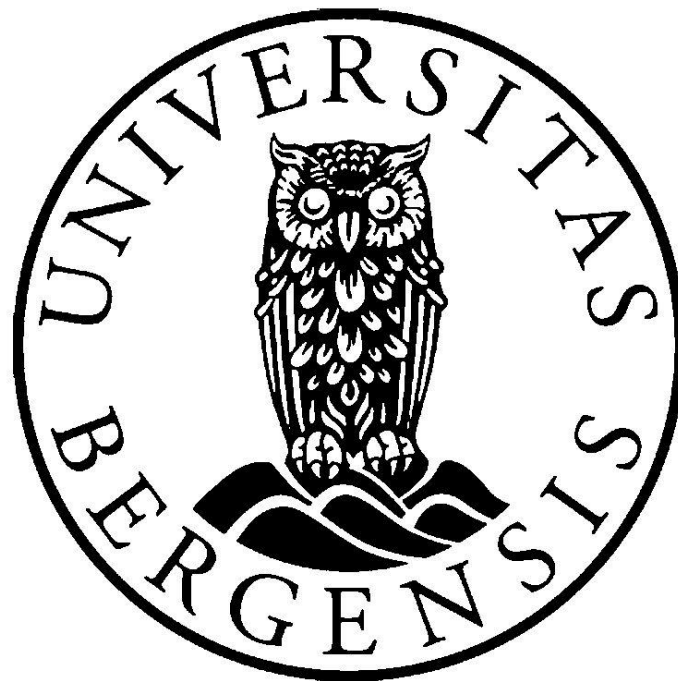Master Thesis in Reservoir Physics

Rheology of Synthetic Polymers in Porous Media

Jørgen Omre Larsen

Centre for Integrated Petroleum Research

Department of Physics and Technology

University of Bergen

June 2014

Acknowledgement

Abstract

This master thesis is written out of the Centre for Integrated Petroleum Research (UNI CIPR) at the University of Bergen (UiB). The aim of this study has been to describe the polymer rheology of the high molecular weight synthetic polymer HPAM 3630S and the lower molecular weight synthetic polymer HPAM 3230S in a linear flow through porous media. The experiments were set up with a pump, two core samples wired in series, two differential pressure gauges, and a backpressure regulator.
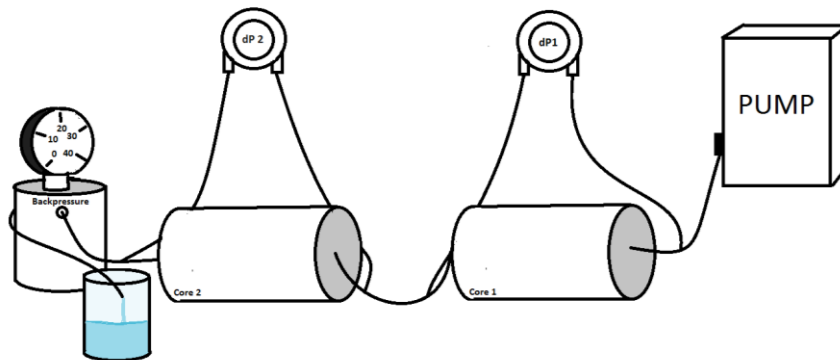
The idea behind the experiment is to inject low and high molecular weight polymer solutions through both core samples and measure the differential pressures at different injection rates at steady state. With this information it is possible, with help from Darcy's Law and a proportionality formula between injection rate and shear rate, to calculate the apparent viscosity and apparent shear rate of the polymer solution in the porous media. The apparent viscosity could then be compared to other apparent viscosities and rheometer measurements.

In the experiments it was found that the rheological behavior of viscoelastic synthetic polymers is different from rheometer measurements. The degree of shear thickening (viscoelasticity) seems to be larger in porous media, a steeper viscosity increase compared to what was expected, especially for the high molecular weight polymer. In the rather short

cores used for injections there was also an evident shear thinning region at injection rates lower than the onset of shear thickening.

In the rheometer data there was found to be a large deviation in viscous properties for high molecular weight and low molecular weight polymers. The low molecular polymer did not only show less viscosity per ppm solution, but also a less shear thinning and shear thickening effect at concentrations where the viscosity at a shear rate of $10s^{-1}$ was nearly identical.

The viscous behavior in porous media showed that the low molecular weight polymer showed a later onset of shear thickening, although more viscous at medium to low injection rates than what to be expected from rheometer results.

The low molecular weight polymer also showed less permeability reduction and less mechanical degradation of the two.

Table of Contents

List of Figures

List of Tables

Nomenclature

Variables

τ	Shear Stress
μ	Viscosity
V	Velocity
y	Distance
$\dot{\gamma}$	Shear Rate
$\dot{\omega}$	Angular Speed
r	Radius
α	Angle or Pore Geometry Constant
R_c	Radius of Cone
R_r	Radius of Cone Truncation
τ_c	Shear Stress on Cone
T_c	Rotational Torque
φ	Porosity
φ_a	Absolute Porosity
φ_{eff}	Effective Porosity
Q	Effective Porosity
k	Absolute Permeability
A	Cross-Sectional Area

L	Length
ΔP	Pressure Loss
τ_w	Shear Stress Acting on a Wall
F_f	Frictional Force
A_w	Area of Wall
B	Pore Geometry Constant
u	Bulk Velocity
F_p	Lost Pressure Force
I	Injectivity
$V(r)$	Velocity Profile in a Tube
R	Tube Radius
V_{avg}	Average Velocity
$\dot{\gamma}_{eff}$	Effective Shear Rate in a Tube
μ_{app}	Apparent Viscosity in Porous Media
μ_N	Viscosity of a Newtonian Fluid
ΔP_N	Pressure Loss in a Newtonian Fluid
ΔP_{n-N}	Pressure Loss in a Non-Newtonian Fluid
$V_{p,avg}$	Average Pore Velocity
Q_{bulk}	Bulk Volumetric Flow Rate
A_{bulk}	Bulk Cross-Sectional Area
$R_{p,avg}$	Average Pore Radius
C	Pore Geometry Factor

Abbreviations

HPAM	Partially Hydrolyzed Polyacrylamide
EOR	Enhanced Oil Recovery
IOR	Improved Oil Recovery
CIPR	Centre for Integrated Petroleum Research
g	Grams
L	Liters
NaCl	Sodium Chloride
$NaHCO_3$	Sodium Bicarbonate
ppm	Parts Per Million
°C	Degree Celcius
WAG	Water Alternating Gas
CO_2	Carbon Dioxide
cP	Centipoise (unit for viscosity)
dP	Differential Pressure
mD	Millidarcy (unit for permeability)
RF	Resistant Factor
2-D	Two Dimensional
3-D	Three Dimensional
PV	Pore Volume
In-Situ	In this Context; In Porous Media

1 Introduction

Petroleum is hydrocarbon molecules that were formed from the remains of prehistoric plants and organisms. Dead plants and organisms were buried under sand, silt and rocks on the sea bottom. New layers of dead organic material were constantly formed. After millions of years with increasing pressure and temperature, the sand, rocks and silt turned into porous source rock and slow-cooked the organic layers into oil and gas. During these years the hydrocarbons migrated upwards in connected pores due to its low density. Like a rising balloon of helium in air. Some of the oil and gas leaked up to the surface of the earth, and some of it was trapped deep within the earth by impermeable rock barriers. This is oil reservoirs. [1]

Human beings use petroleum for energy and as materials for different products. Petroleum is incredible valuable, due to its high energy density. With oil and gas being insanely important to human beings, the demand for petroleum will continue to increase as both energy use and world population increases.

We know that petroleum fluids are trapped in reservoirs that are made of porous rock deep beneath the surface. All of the overlaying rock, sand, and water make for a high fluid pressure in the reservoir. This means we can drill a well down into the reservoir, and start producing naturally when we penetrate the cap rock. This is called primary recovery. Maintaining the reservoir pressure by injecting water or gas in a separate well is called secondary recovery. The last recovery method is called Enhanced Oil Recovery (EOR) or tertiary recovery, and consists of injecting foreign compounds (polymers, surfactants, gas, CO_2, foam, WAG) into the reservoir to decrease the amount of residual oil or to speed up the production. [2]

The expected recovery factor on the Norwegian Continental Shelf is 46% for oil fields and 70% for gas fields. Globally, the expected recovery factor for oil fields is estimated at 22%. With petroleum being a nonrenewable resource and having the world's increasing energy demand in mind, we have to explore and improve current recovery methods. [3]

This master thesis is focused towards single phase synthetic polymer injections into porous media and their rheological properties.

Polymer injection is an EOR method where polymer molecules are added to the injection water. This increases the viscosity of the injection water and reduces the rock's permeability to water. [4]

The objective of this study is to better understand how the viscosity of the synthetic polymers HPAM 3630S and HPAM 3230S changes in porous media at different injection rates. HPAM 3630S is a high molecular weight polymer, and HPAM 3230S is a lower molecular weight polymer.

My personal goal for this thesis is to present the theory, experiments and results in a clear and understandable way. I will also try to discuss some more advanced theoretical ideas that have been discussed in previous literature.

The thesis was given by Professor Arne Skauge.

2 Theory

The theory described here is a basic theoretical background for the subjects and experiments in this thesis. Parameters and theories not relevant or considered in the experimental work might not be presented or explained. Some explanations might be subjective in some form, but it is all related to the experimental work and my personal understanding of these complex subjects.

2.1 Fluid Properties

A fluid is a substance that will flow or deform when put under shear stress. Their molecules changes positions under applied force. The more used definition is that fluids are liquids and gases. All of the valuable hydrocarbons down beneath us are fluids. Their properties are therefore important parameters in reservoir production. In EOR injections, the properties of the injected fluids are also crucial.

2.1.2 Viscosity

Viscosity is the friction between the molecules in a fluid when stress is applied. It is more generally explained as the fluid's resistance to flow or deform. Oils generally have a higher viscosity than water; they have more internal friction and thus resistance to flow. Gases flow very easily, thus they have very small viscosities. Viscosity is dependent on temperature, pressure and often the applied shear stress. Increasing temperature will decrease the viscosity of liquids and increase the viscosity of gases. This can be explained by molecular physics, where the cohesive forces between the molecules of a liquid decreases as the thermal energy increases and molecules become more mobile. The friction between the molecules has been reduced. The molecules in a gas will have more kinetic energy by increasing temperature and the frequency of intermolecular collisions will increase. This leads to more resistance and friction internally in the gas when forces are applied. [7] Higher pressure will result in increasing viscosity for both liquids and gases, except for water. Note that the effect of pressure often can be neglected. Viscosity can be measured by a

viscometer or a rheometer and has the unit Centipoise [cP] or Pascal Second [Pa·s]. One Pascal Second equals 1000 Centipoise. Water at 20°C has a viscosity of 1cP. [9]

2.1.3 Rheology

Rheology is defined as the study of flow and deformation of materials under applied stress. This can be solids, liquids or gases. In this thesis, the rheology term is focused towards liquids and the study of polymer viscosity under applied shear stress. The viscosity of a fluid can be altered by increasing or decreasing the shear rate or strain rate on non-Newtonian fluids. A fluid where the viscosity is constant at any given shear rate is called Newtonian fluids, for example water, oil and air. Most fluids we encounter in food, chemicals and biology are non-Newtonian.

Non-Newtonian fluids are typically divided into:

- Shear thinning fluids (pseudoplastic fluids)
- Shear thickening fluid (dilatant fluids)
- Bingham plastic fluids
- Thixotropic fluids
- Rheopectic fluids

Thixotropic fluids and rheopectic fluids are time dependent; they change viscosity with constant shear rate over a given time. Thixotropic fluids will have thinning properties after a given time of constant shear rate, for example mayonnaise or thread locking fluid ("Loctite"). Rheopectic fluids will show thickening properties after a given time, with cream being a great example. Bingham Plastic fluids (pseudoplastic liquid with yield point) shows flowing abilities only when higher yield shear stress is applied. Mayonnaise and ketchup are Bingham Plastics because they do not flow when only acted upon gravity and flow under higher shear stress. The viscosity of pseudoplastic and plastic liquids will decrease with increasing shear forces, and shear thickening fluids will behave in the opposite way. Examples of shear thinning fluids are paint, blood, polymers, drilling fluid etc. Examples of shear thickening fluids, also called dilatants, can be cornstarch mixed with water or certain types of body armor. Dilatants will behave as a solid when applied under a great shear stress, for example shot with firearms. [9]
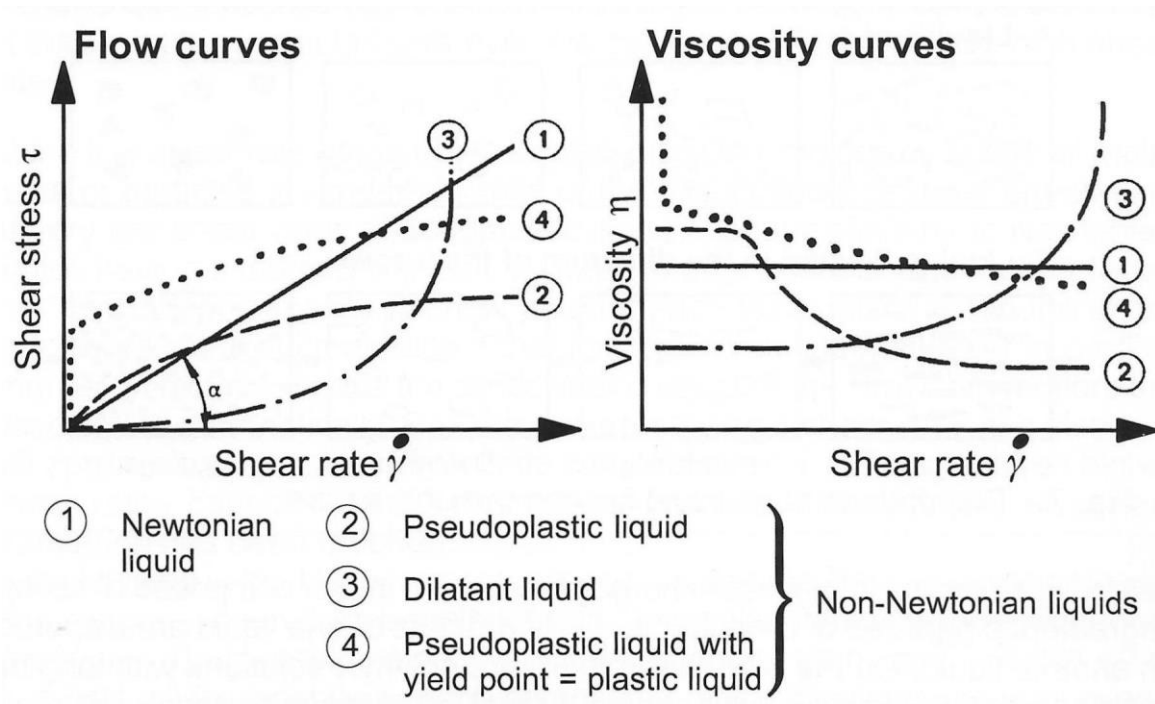
Figure 1: Flow and viscosity curves for different types of fluid. [8]

It is worth noting that these fluid types are idealizations, and the rheology is generally more complex. [13]

2.1.4 Shear Thinning Fluids

Shear thinning fluids, most polymers, generally have Newtonian regions at low and high shear rates. This can be explained by looking at the fluid molecules. Shear thinning fluids generally have bigger molecules with higher molecular weight than Newtonian fluids. At rest or at very low shear rates, these large molecules "float" around in different directions causing a high friction between them, i.e. higher viscosity. This is seen as the low-shear plateau.
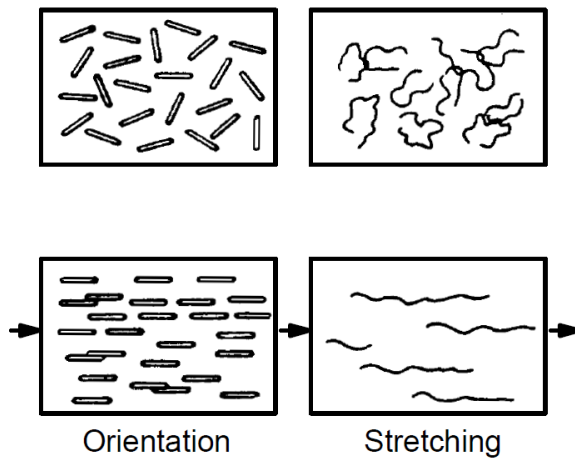
Figure 2: Orientation and stretching of fluid molecules at rest and during flow. [8]

When the shear forces are high enough to break this molecule arrangement, the molecules tend to rearrange to the flow direction causing less friction between them. This rearrangement process is seen as the shear thinning region. When all of the molecules are aligned and arranged in the flow direction the high shear plateau has been reached. The total friction between the molecules reaches its lowest level. [14]
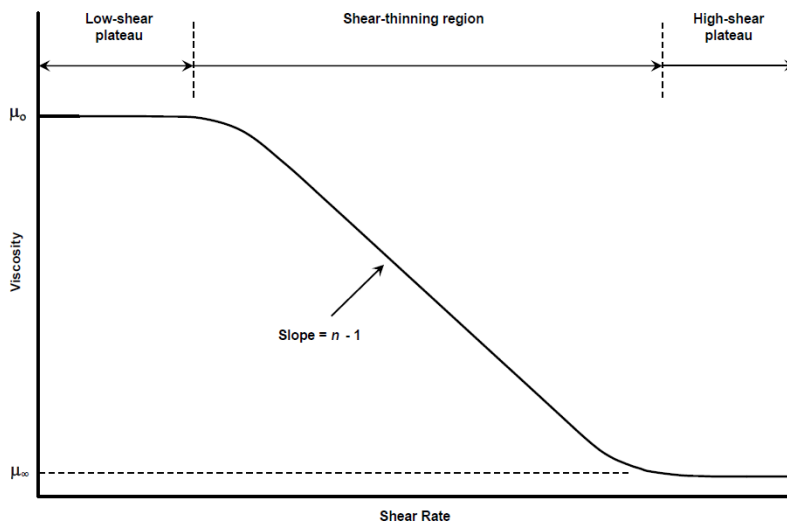
Figure 3: Carraeu model for shear thinning fluids. [13]

This rheological model is called the Carraeu model and is one of many mathematical models interpreting non-Newtonian fluid behavior.

19

2.1.5 Viscoelastic Fluids

Viscoelastic fluids have both viscous and elastic properties. All fluids have viscous properties, i.e. they flow under applied forces like gravity or bigger stresses. Some fluids have elastic properties; their molecules can be stretched under shear stress and return to their original form when the stress is removed. Just like a rubber band. These rubber band molecules can have a big impact on the viscosity at different shear rates and thus a big impact on the viscosity of the fluid that is being injected into porous media. Many biological fluids have elastic properties like blood, mucus and saliva. You can stretch the mucus coming out of your nose and once you let go the mucus will return to its original form. Elastic fluids have the ability to store and release energy. The polymers used in this thesis, HPAM 3630S and 3230S, also have elastic properties depending on the concentration.

Shear thinning viscoelastic fluids have unique viscosity properties at high shear rates. As explained with inelastic shear thinning fluids, the viscosity decreases as the molecules become more and more arranged in the flow direction until all the molecules are aligned. If the shear rate continues to increase, the elastic large molecules will begin to stretch (figure 2). Thus, the resistance to flow will increase as there are two friction forces stealing energy from the flow, friction between the molecules and the stretching resistance of every molecule. This is seen as a shear thickening zone. The flow of stretching molecules is sometimes referred to as elongational flow. [14]
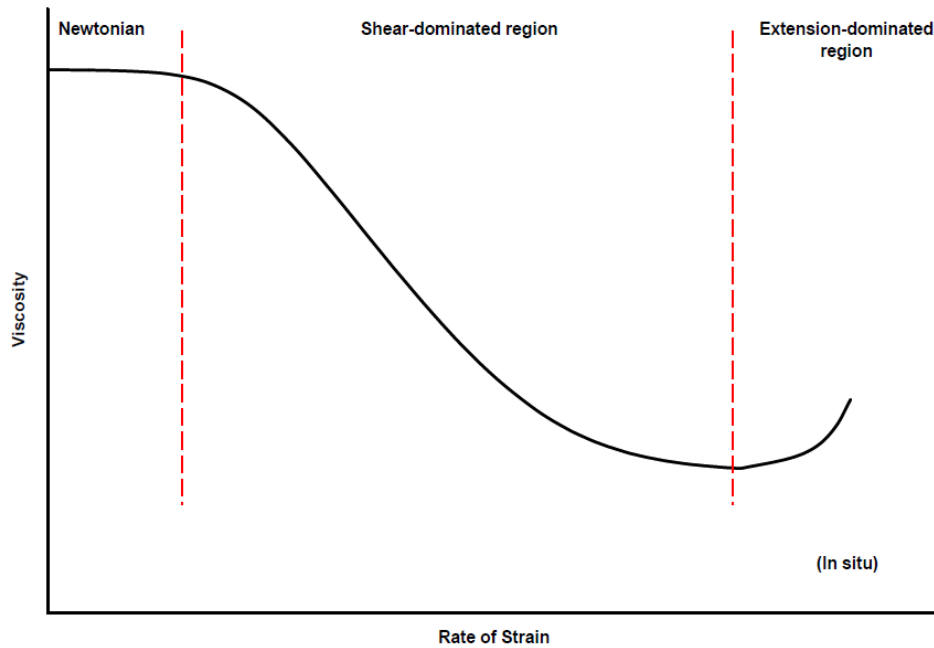
Figure 4: Viscoelastic viscosity curve, typical for HPAM. [13]

If the shear rate continues to increase beyond the shear thickening zone, the molecules will eventually start breaking which causes a viscosity decrease. This is called mechanical degradation. The rheological properties of the fluid are now altered forever.

There are several phenomenon linked to viscoelastic fluids such as rod climbing (Weissenberg effect), die swell and open siphon effect.
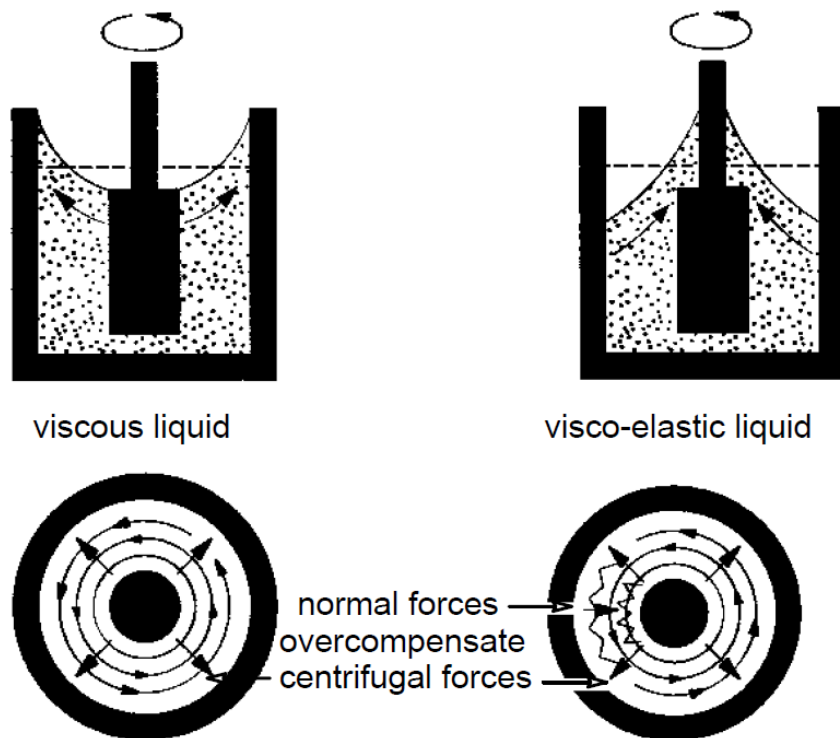
Figure 5: Illustration of the Weissenberg effect (climbing rod effect). [8]

Here is a figure demonstrating the rod climbing effect. When a viscoelastic fluid is being stirred by a rotor shaft the fluid will be pulled towards the shaft and climb upwards. This phenomenon can be explained by the fact that viscoelastic fluids always try to escape to a state with less stretching, i.e. their original form. The molecules are more stretched on the outer layers due to centrifugal forces and they try to escape inwards towards the lower shear stress. When it "gets crowded" towards the rotor shaft the molecules tend to escape upwards. [8]

These theories also apply in the die swell phenomenon, which is when a fluid expands when flowing out of a small tube. This phenomenon is closely related to viscoelastic expansion in porous media flow when a fluid is entering a larger pore.
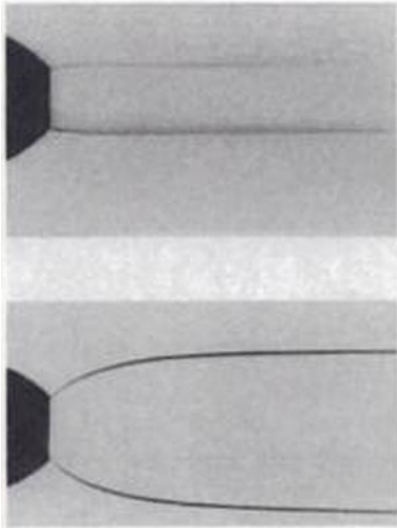
Figure 6: Illustration of the die-swell effect. [15]

The correlating factor here is the memory of the fluid and the wish to return to its original shape. Just like a rubber band would like to return to a relaxed position. The viscoelastic fluid wants to be relaxed. An important parameter for viscoelastic fluids is relaxation time. Relaxation time is the time it takes for a fluid to return to its desired shape after being stretched. This introduces time as an important parameter, especially when there are jumps in shear rate (strain rate).
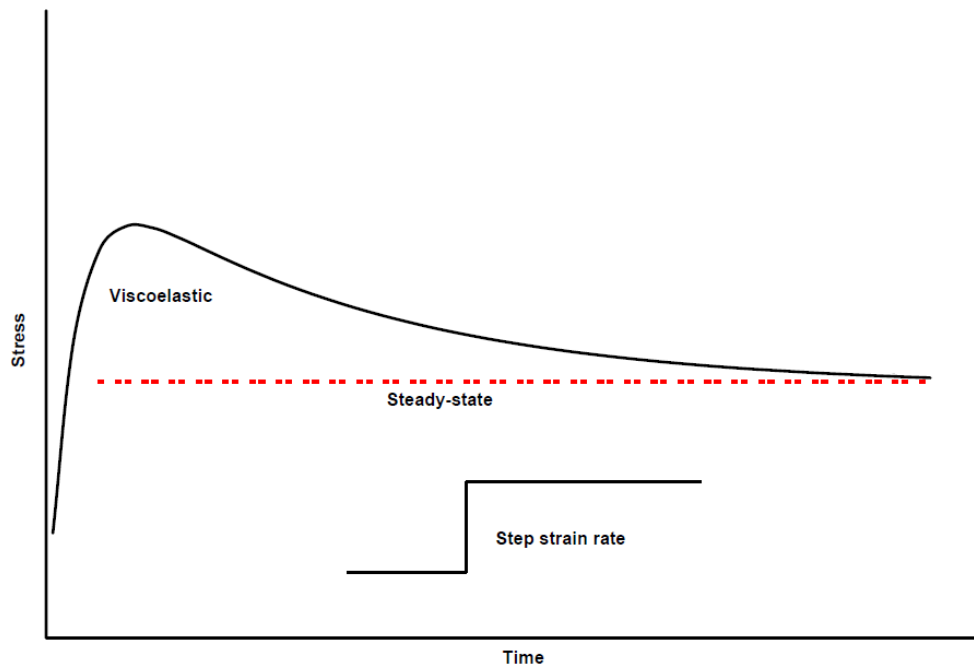
Figure 7: Inflicted stress vs. time after a step up in strain rate for viscoelastic fluids. [13]

An increased jump will increase and then decrease the viscosity (or stress) as a function of time depending on the relaxation time, degree of elasticity and jump magnitude. This is given that the shear rate reaches the fluids shear thickening (elastic) properties. Imagine a car pulling a trailer with an elastic tow rope. If the car suddenly made a speed step increase it would take time before the tensional forces in the rope would approach a steady state due to the elasticity of the rope. The relaxation time in this case would be the time from maximum tensional force to the steady state tensional force.

2.1.6 The Rheometer

A rheometer is a laboratory device that can measure fluid parameters, such as viscosity, in response to applied forces. The rheometer can measure more parameters, such as viscosity at different shear rates, than the simpler viscometer. The measurement of viscosity requires understanding of basic parameters in a laminar flow model case. Laminar flood is when a fluid flows in parallel layers without disruption between the layers. An easy and understandable model is laminar flow between two parallel flat plates for Newtonian fluids.

24
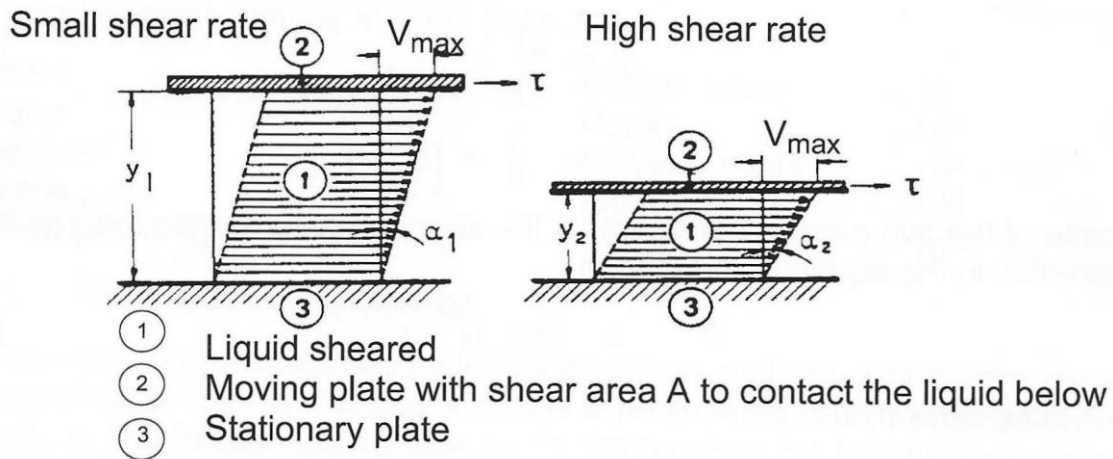
Figure 8: Parallel plate flow model used to define viscosity for Newtonian fluids. [8]

The upper plate is moving at a constant velocity *V*, applying a shear stress on the fluid between the layers. This model assumes a no slip condition along both plates, so called adhesion. This means that the fluid molecule layer closest to the upper plate is sticking to the plate surface, ergo having the same constant velocity *V* as the plate. This basically means that the friction between the plate and the upper molecule layer is greater than the friction between the upper molecule layer and the layer beneath. In some cases this is not true in a practical experiment, especially using certain fats and greases. However, if the friction, i.e. the viscosity between the fluid layers, is high, the velocity *V* of the plate will be smaller at equal applied shear stress. Visa versa applies with smaller viscosities. The velocity of the fluid molecules will decrease the closer you get to the bottom stationary plate. The velocity of the bottom layer of molecules will consequently be zero. Newton expressed a basic law of viscometry describing the flow behavior of an ideal liquid. [8]

$$\tau = \mu \cdot \frac{dV}{dy} = \mu \cdot \dot{\gamma} \qquad\qquad (2.1.1)$$

Where shear stress, τ, is defined as;

$$\tau = \frac{Force}{Area} = \frac{N}{m^2} = Pa \tag{2.1.2}$$

And the shear rate is defined as;

$$\dot{\gamma} = \frac{dV}{dy} = \frac{m/s}{m} = s^{-1} \tag{2.1.3}$$

Using these equations the viscosity can be defined;

$$\mu = \frac{\tau}{\dot{\gamma}} = \frac{Pa}{s^{-1}} = Pa \cdot s \tag{2.1.4}$$

For Newtonian fluids the viscosity is constant at different shear rates. This means that the applied shear stress is proportional to the shear rate. Since the distance *y* between the plates is constant, the shear rate represents the velocity of the upper plate in figure 8. For non-Newtonian fluids the viscosity is not constant, it is a function of shear rate. [17]

$$\tau = \mu(\dot{\gamma}) \cdot \dot{\gamma} \tag{2.1.5}$$

In this case, the velocity profile is not linear. The microscopic viscosity decreases (shear thinning) or increases (shear thickening) from the moving plate as a function of y. This is because the shear forces acting on the fluid is larger towards the moving plate. The shear rate between the plates (equation 2.1.3) is also a function of y because the velocity profile

no longer is linear. For every amount of shear stress applied to the moving plate there might be a new and different shaped velocity profile depending on the rheological properties of the fluid.
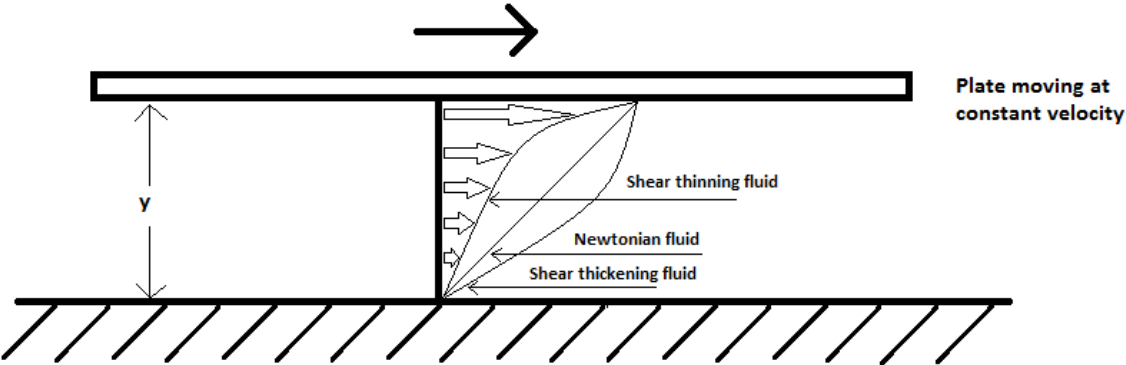
Figure 9: Parallel plate flow model for non-Newtonian fluids.

The shear stress dragging the molecule layers in the flow direction is also changing as a non-linear function of y. However, the shear stress in equation 2.1.5 is only dependent on the friction between the uppermost flowing fluid molecule layer and the no-slip molecule layer. This friction is dependent on the friction between the other molecule layers. It is this friction that resembles the resistance of the fluids flow, i.e. its viscosity. Since it is pointless and practically impossible to measure the molecular level viscosity in a non-Newtonian fluid, we have to measure the resistance to flow on a macroscopic level, and thus measure the effective viscosity based on the laws and definitions for Newtonian fluids. The effective (shear) viscosity for a non-Newtonian fluid is defined as the equivalent Newtonian viscosity that results in the same shear stress at a surface at equal volumetric flow rates.

The laminar flow between parallel plates model is the principle for the rotational rheometer used in this thesis. The geometry used was a truncated cone and plate system, where the cone rotates and creates a fluid flow over a stationary plate. The cone will simulate the upper moving plate in figure 8, shearing the liquid underneath. The rheometer will apply a

rotational force on the cone, acting as a shear stress on the fluid. The resistance the rotational movement receives from the fluid represents the viscosity, and the rotational speed at the given shear stress represents the shear rate. The distance between cone and plate is kept constant at all times.

Rc = Outer radius of cone
α = Cone angle
R_T = Truncation radius
a = Height of removed tip

test sample
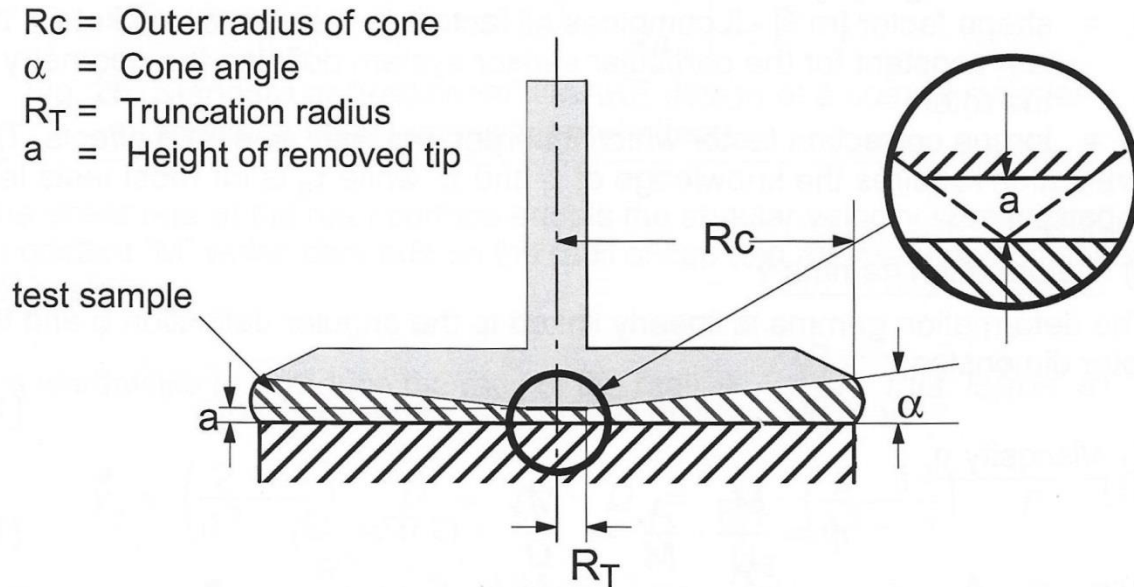
Figure 10: Illustration of a rotational cone and plate rheometer. [8]

A cone is used instead of a flat circular plate because the shear rate is constant at any point on the cone surface.

$$\dot{\gamma} = \frac{dV}{dy} = \frac{Linear\ speed}{Distance\ to\ the\ plate} = \frac{\dot{\omega} \cdot r}{r \cdot \tan(\alpha)} = \frac{\dot{\omega}}{\tan(\alpha)} \qquad (2.1.6)$$

r is radius and $\dot{\omega}$ is angular velocity. The truncation of the cone is not taken into consideration.

Most cone and plate systems use a truncated cone because larger errors might occur due to possible wear and errors at the tip, especially when testing dispersions. Truncation minimizes the probability of larger errors for the prize of a smaller truncation error which is about 1% for R_c=30mm and R_t=3mm. [8]

28

To calculate the shear stress we can divide the cone into several small horizontal surface layers, every one of them having a radius r and the height h.
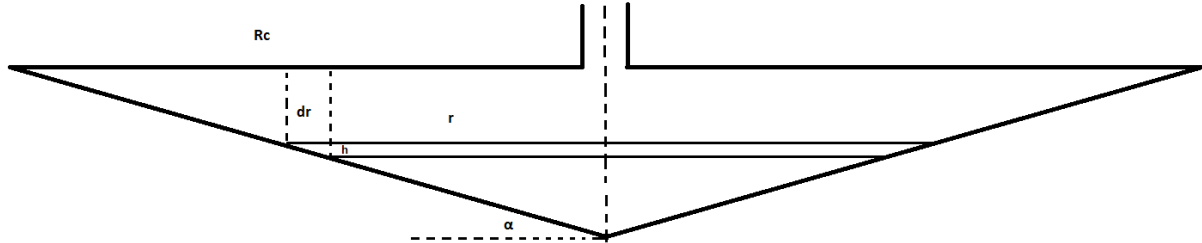
Figure 11: Illustration of the mathematical variables for integration of the shear stress on a cone.

From this figure we see that $h = dr/\cos \alpha$. The surface area of each layer is consequently $2\pi r \cdot \dfrac{dr}{\cos\alpha}$. We can now derive an expression for the total shear stress acting on the cone using simple integration of the shear stress for each layer area from $r = 0$ to $r = R_c$.

$$\tau_c = \frac{F}{A} = \int_0^{R_c} \frac{\frac{T_c}{r}}{2\pi r \cdot \frac{dr}{\cos(\alpha)}} = \frac{\cos(\alpha) \cdot T_c}{2\pi \cdot \int_0^{R_c} r^2 dr} = \frac{3\cos(\alpha) \cdot T_c}{2\pi R_c^3} \qquad (2.1.7)$$

T_c is the rotational torque acting on the cone spindle. The viscosity can be defined using equation (2.1.2).

$$\mu = \frac{\tau_c}{\dot{\gamma}} = \frac{\frac{3\cos(\alpha) \cdot T_c}{2\pi R_c^3}}{\frac{\omega}{\tan(\alpha)}} = \frac{3\cos(\alpha) \cdot T_c \tan(\alpha)}{2\pi R_c^3 \omega} \qquad (2.1.8)$$

The rod climbing effect described earlier also plays a role in the cone and plate rotational rheometer when testing viscoelastic fluids. Since the shear stress is higher at a larger radius, the molecules try to escape to a lower radius where the molecules are being stretched less.

Since there is no room for more molecules inwards the molecules tries to escape upwards creating a normal stress acting on the cone. Note that this only happens at sufficiently high shear rates when the molecules begin to stretch at the shear thickening region. The normal stress will increase with shear rate until the fluid suddenly escapes from the gap and upwards the outer rim of the cone or until the fluid is exposed to mechanical degradation. [8]

Another often used geometry for rotational rheometers is the coaxial cylinder, a rotating cylinder in a bigger cylinder filled with a sample of the fluid. It is also called the double gap geometry. This geometry is better suited for lower concentrations, as it has a bigger surface area and consequently more rotational friction per unit viscosity, i.e. more accurate readings at low viscosities. [8]

2.2 Rock Properties

All rock samples have a different set of properties, and there are several layers of different rock within a reservoir. In petroleum engineering these properties are very important to create good mathematical models and predictions. Measurements of these parameters are done by core analysis tests and well logging.

2.2.1 Porosity

Porosity is defined as a measure of the storage capacity that is capable of holding fluids in a rock. It is expressed as a fraction of the bulk volume. [5]

$$\varphi = \frac{Pore\ volume}{Bulk\ volume} \qquad (2.2.1)$$

This parameter is important in oil and gas reservoirs because it tells us the potential of hydrocarbon volume in the field. Some void spaces in the rock are isolated from other void spaces. This leads to two different types of porosity, absolute porosity and effective porosity. Absolute porosity is defined as the total pore volume as a fraction of the bulk volume. [5]

$$\varphi_a = \frac{Total\ pore\ volume}{Bulk\ volume} = \frac{Bulk\ volume - grain\ volume}{Bulk\ volume} \qquad (2.2.2)$$

The effective porosity is the interconnected pore space as a fraction of the bulk volume. This is the pore space where fluid can flow. This porosity parameter is used in reservoir engineering and also used in the experimental work of this thesis. [5]

$$\varphi_{eff} = \frac{Interconnected\ pore\ volume}{Bulk\ volume} \qquad (2.2.3)$$

2.1.3 Absolute permeability and Darcy's law

Permeability is the capacity and ability of a porous medium to have fluids flow through the interconnected pore space. It behaves like an electrical conductivity in an electrical flow. Higher permeability means less resistance for the fluid to flow through the pores. This parameter was first defined mathematically by Henry Darcy in 1856. [5]

Darcy's law:

$$Q = \frac{k \cdot A}{\mu} \cdot \frac{\Delta P}{L} \qquad (2.2.4)$$

Where Q is the volumetric flow rate, k is absolute permeability, A is cross sectional area, ΔP is the differential pressure, L is the length and μ is the viscosity of the fluid. Following conditions for this equation must be satisfied:

- Linear, laminar and horizontal flow
- Incompressible fluid
- No chemical reactions between fluid and rock
- The porous medium must be 100% saturated with one single fluid
- Constant viscosity

The most used unit for permeability (k) is Darcy (D), but m^2 is often used in calculations. Equation (2.2.4) can be modified for different flow angles, but the same conditions have to be met. [6] In this thesis, Darcy's law will be used to calculate the apparent viscosity, i.e. the average of the effective viscosities in the porous media weighted by flow rate, in different core samples as well as the water permeability of the porous media.

Darcy's law can be derived using the total frictional forces acting on a fluid through a porous media sample.

When a fluid flows through a capillary tube or a pore the fluid velocity is zero at the tube walls due to the no-slip condition. The velocity increases towards the center of the tube where it reaches its maximum speed. [12]
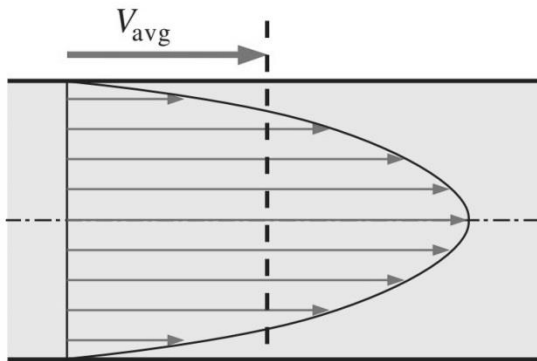
Figure 12: Velocity profile for a Newtonian fluid flowing in a tube. [12]

The frictional forces from the walls are indeed shear stress acting on the fluid. This shear stress between the fluid molecules decreases towards the center of the tube, the shear forces slows down the fluid velocity like brakes on a car. The amount of shear resistance or braking power depends on the fluid viscosity, i.e. the friction between the fluid molecules. Lower viscosity results in a higher average velocity. This is in principle how a fluid flows through pores in a porous medium. One must remember that the pores in a rock have different shapes, sizes and directions. The principle of friction force or shear stress caused by the all the pore walls inside still apply. If we take a look at a simple core flooding experiment at steady state flow we can use the definitions in equation (2.1.2) and (2.1.1) to have a look at the forces acting on the injecting fluid. Gravity is neglected. [6]
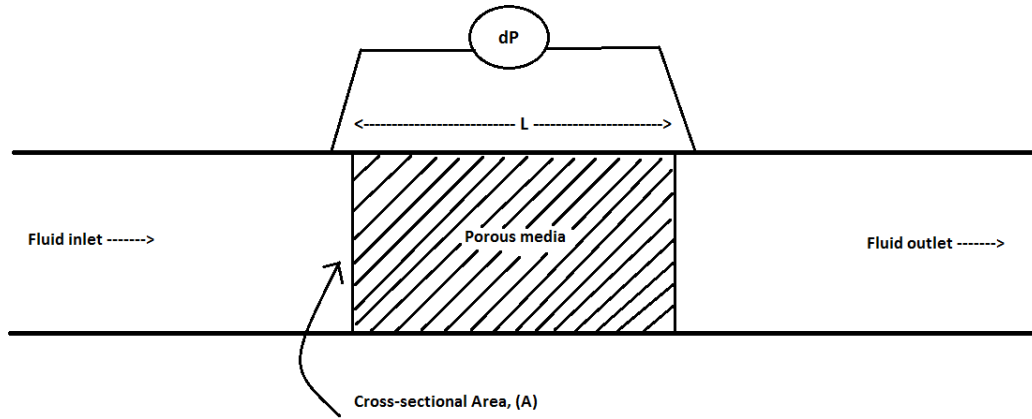
Figure 13: Illustration of a linear flow through porous media.

The total shear stress acting on the pore walls;

$$\tau_w = \frac{F_f}{A_{wall}} = \mu \cdot \dot{\gamma}_{app} \tag{2.2.6}$$

F_f is the total frictional force creating a pressure drop, A_{wall} is the total interconnected pore wall area, μ is the viscosity and $\dot{\gamma}_{app}$ is the apparent fluid shear rate in the porous media. Since the apparent shear rate is proportional with the fluid velocity at the core inlet (the bulk velocity u) and the total pore wall area A_{wall} can be said to be proportional with the total core volume $A \cdot L$ given constant and homogeneous rock properties, we can express the total frictional force as;

$$F_f = A_{wall} \cdot \mu \cdot \dot{\gamma}_{avg} = BAL\mu u = B\mu QL \tag{2.2.7}$$

B is a proportionality constant dependent on the pore geometry. [6] If we assume that the pressurized fluid enters a total pore cross-sectional area of $\varphi \cdot A$, the pressure force lost by the friction can be written;

$$F_p = \Delta P \cdot \varphi \cdot A \qquad\qquad (2.2.8)$$

As the fluid flows in a steady state, we have;

$$F_p = F_f$$

$$\Delta P \varphi A = B \mu Q L$$

$$\rightarrow Q = \frac{\frac{\varphi}{B} A}{\mu} \cdot \frac{\Delta P}{L}$$

The energy from the frictional force transmitted by the pore walls is transformed into heat. From here Darcy defined the absolute permeability $k = \frac{\varphi}{B}$, resulting in the infamous Darcy's law (2.2.4);

$$Q = \frac{kA}{\mu} \cdot \frac{\Delta P}{L}$$

2.3 Polymer Injection

2.3.1 Enhanced Oil Recovery

Enhanced Oil Recovery (EOR) is linked to the use of unconventional recovery methods, and is defined as oil recovery by injecting materials not normally present in the reservoir. Examples of EOR methods:

- Polymer flooding

- Surfactant flooding

- Foam injection

- CO_2 injection

- WAG injection (Water-Alternating-Gas)

- Low Salinity injection

- Thermal methods

- Microbial Increased Oil Recovery (MIOR)

- Diversion techniques

All EOR methods are injected through at least one separate injection well, often at a greater distance from the production wells. Regular water injection is not classified as an EOR method, as water is normally present in the reservoir. EOR, water injection and all other methods that are intended to improve oil recovery or accelerate the production are defined in a broader manner as Improved Oil Recovery (IOR) methods. [10]

2.3.2 Polymer Flooding

The basics of polymer flooding start with the basics of water injection. The purpose of a water flood is to maintain the reservoir pressure and displace the reservoir oil. [10]
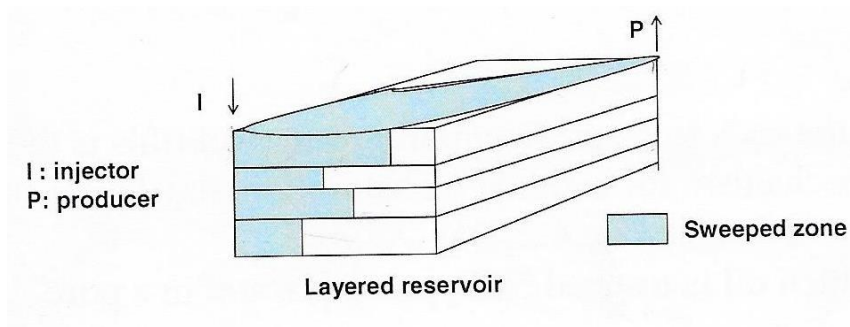
Figure 14: A simple reservoir model during water injection. [10]

This figure shows a typical water injection in a simple reservoir model. The water is being injected from the injection well at a high pressure and thus flowing towards the production well having a smaller pressure.

Polymer flooding is injection of water mixed with polymer molecules to increase the viscosity of the water. This leads to higher a viscous force at equal injection rates and therefore reduced water mobility in the reservoir. The purpose is to improve the sweep efficiency in the reservoir. The sweep efficiency is how fast or effective the injected fluid flows through the entire reservoir volume. Poor sweep efficiency leads to early water breakthrough and slower oil production after breakthrough resulting in economic losses. The reason for poor sweep efficiency can either be unfavorable mobility ratio between oil and water or excessive reservoir heterogeneity. [17]

Poor mobility ratio:
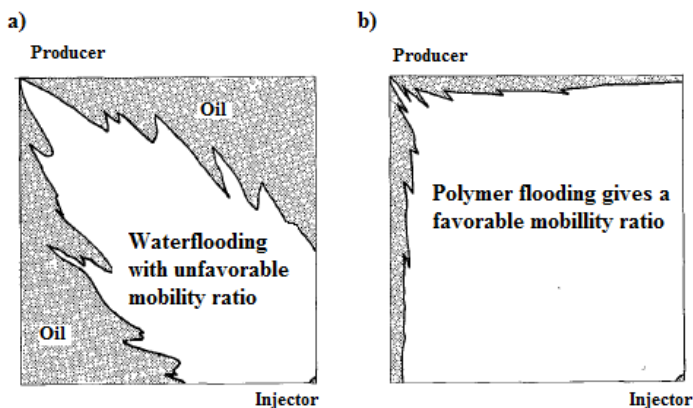
Figure 15: Illustration of sweep efficiency for unfavorable and favorable ratio between the mobility of injection water and oil. [17]

Excessive reservoir heterogeneity:

$$k_2 > k_3 > k_1$$
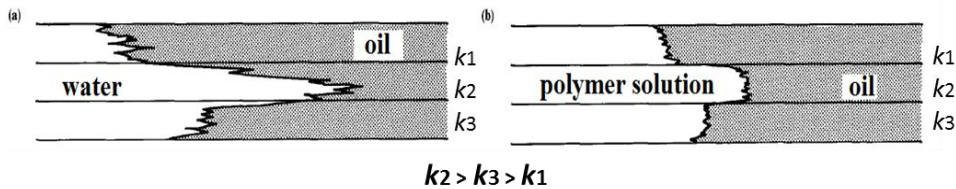
Figure 16: Illustration of sweep behavior in a heterogeneous reservoir model for mobile injection water and less mobile polymer flood. [17]

2.3.3 Polymer Retention

Polymer retention is interactions between the porous medium and the polymer molecules causing the polymer to be retained by the rock. This does not only mean a loss of polymer molecules but also an alteration of rock properties. Retention is defined as the cause of permeability loss after polymer injection. The polymer molecules can either be absorbed to the pore surface, trapped mechanically by narrow channels or trapped hydro dynamically in stagnant zones. [17]
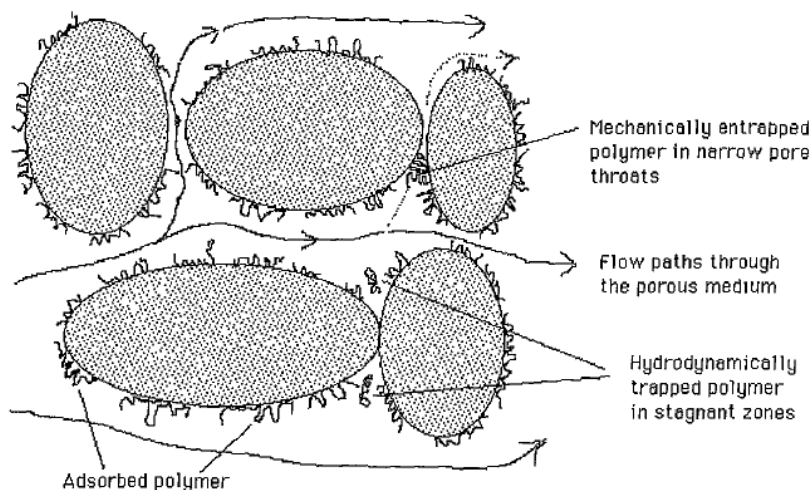
Figure 17: Retention mechanisms in porous media. [17]

2.3.4 Hydrolyzed Polyacrylamide (HPAM)

HPAM is a synthetic polymer with a flexible chain structure. It has viscoelastic properties that give HPAM solutions unique properties in terms of shear viscosity and viscous properties in porous media. [10] The viscoelastic behavior can certainly behave as an advantage in a heterogeneous reservoir compared to non-viscoelastic polymers because the shear thickening effect will decrease the mobility of the polymer even further in high permeable zones due to a higher shear rate. [17]
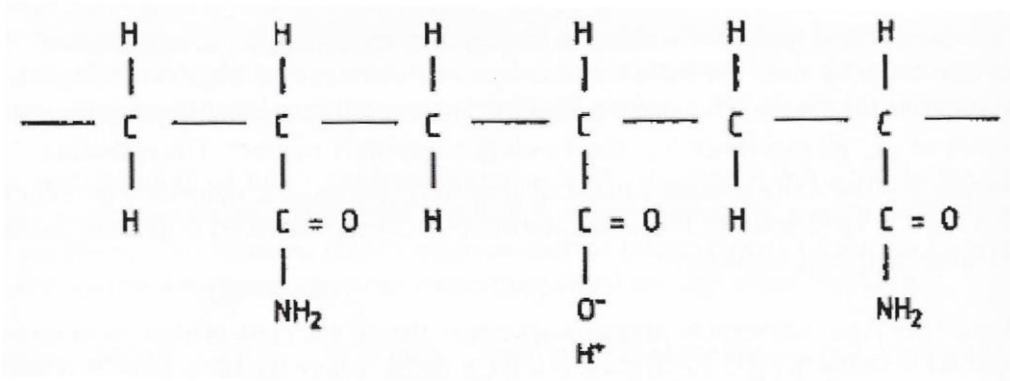
Figure 18: Molecular structure of HPAM (partially hydrolyzed polyacrylamide). [10]

There are several different HPAM chain molecules that can be used to create polymer solutions. In this thesis, HPAM 3630S and 3230S will be used in the experimental work. Generally HPAM 3630S have bigger and longer molecules giving higher viscosity and more viscoelastic properties than of the HPAM 3230S of the same concentration. The magnitude of difference does also depend on concentration.

39

2.3.5 Single Phase Polymer Flow in Porous Media

This is the theory behind the porous media injections in the experimental work. It is a complicated subject due to the very complex fluids flowing through very complex pore channels. In polymer flooding on a reservoir scale it is important to know the polymers viscosity in the rock and thus its resistance to flow through the rock at different injection rates. An important parameter is the injectivity of a fluid.

$$I = \frac{Q}{\Delta P}$$

(2.3.1)

Q is the volumetric injection rate, ΔP is the differential pressure between two reference pressures and I is the injectivity. The injectivity is important because an EOR flood needs a certain level of volumetric injection to sweep the reservoir efficiently. If the injectivity is low, the limitations in pumping equipment and potential fracturing might demand another injection well to meet the sufficient effectiveness of the sweep. [10]

Since the differential pressure (and injectivity) is a direct consequence of the viscous forces (friction forces), it is important to study the viscosity of polymers in single phase flow in porous media. The viscosity of polymers in porous media also plays a big role in the sweep efficiency of an oil reservoir because increased water viscosity decreases its mobility and ultimately leads to the goal of polymer injections, better sweep efficiency and a faster production.

To understand the flow through individual pore channels a capillary tube can be used as a pore approximation. The velocity, viscosity and shear rate profiles for Newtonian fluids in a capillary tube are rather simple equations based on viscosity and volumetric rate. This is because the viscosity is constant throughout the profile in a tube as well as in a pore in a porous medium. When the flowing fluid is non-Newtonian the equations become a lot more complex, and really just a simplification of the actual flow profile based on different mathematical models of how the viscosity differentiates under different shear rates.
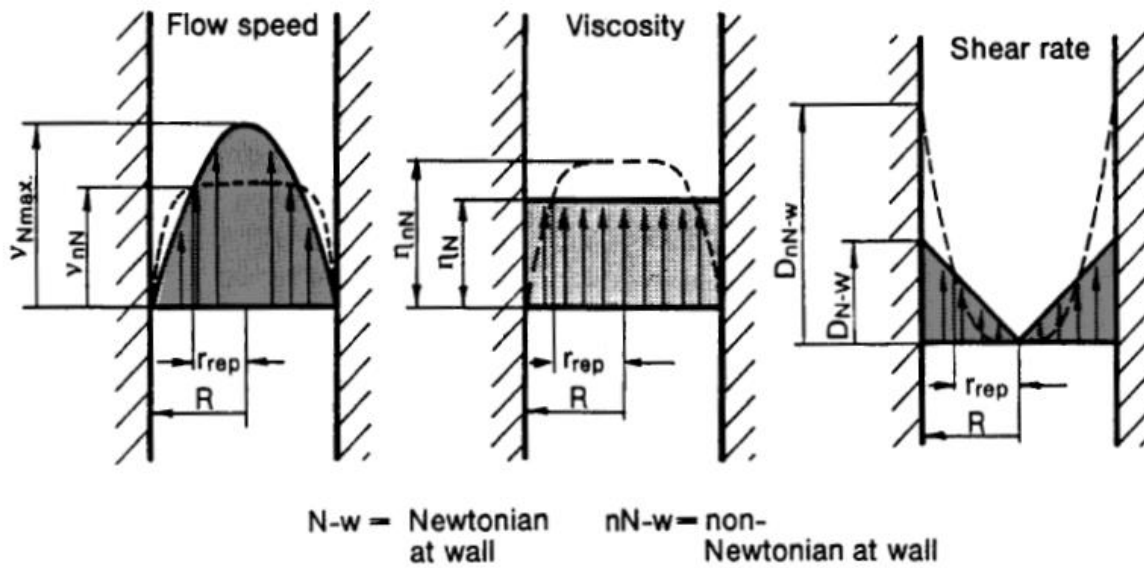
Figure 19: Different flow profiles in a capillary tube for Newtonian and shear thinning non-Newtonian fluids. [8]

In this figure different flow profiles for a Newtonian fluid and a shear thinning non-Newtonian fluid are displayed. Note that the figure only displays the 2-D profiles and that the profiles need to be weighed by the increasing circular area to calculate the average values and 3-D volume. The shear rate profile is a direct result of how much the velocity increases in that particular point (equation 2.1.3). Given constant capillary radius, the velocity profile is dependent upon injection rate and fluid properties, i.e. how the viscosity behaves upon shear stress.

The shear stress acting on the walls in capillary tube of length L, radius R and pressure loss ΔP can be expressed as;

$$\tau_w = \frac{F_{friction}}{A_{wall}} = \frac{\Delta P \cdot \pi R^2}{2\pi R \cdot L} = \frac{R}{2L} \cdot \Delta P \qquad (2.3.2)$$

If we introduce the variable r as the radial position and correlates to equation 2.1.1 we find that the shear rate must be set as negative because the velocity at the surface "delivering" shear stress to the fluid is zero. This is opposite to the parallel plate model.

$$\tau_w = -\mu \frac{dV(r)}{dr} \qquad\qquad (2.3.3)$$

Equation 2.3.2, using the variable *r* instead of R, can be substituted into equation 2.3.3. Solving this differential equation by integration gives us the velocity profile V(r) of a Newtonian fluid.

$$V(r) = \frac{R^2}{4L\mu}\Delta P(1 - \frac{r^2}{R^2}) \qquad\qquad (2.3.4)$$

The average velocity in the 3-D capillary can be found by calculating the volume of the velocity profile divided by the cross-sectional area. The volume is found by integration of the velocity profile weighted by the increasing circumference. The velocities at a higher radius have more impact on the average value because there are more fluid particles due to the larger circumference.

$$V_{avg} = \frac{\int_0^R V(r)\cdot 2\pi r dr}{\pi R^2} = \frac{R^2}{8L\mu}\Delta P \qquad\qquad (2.3.5)$$

Since the injection rate is the average velocity times the cross-sectional area, the volume of the velocity profile is equal to the injection rate.

$$Q = V_{avg} \cdot \pi R^2 = \int_0^R V(r) \cdot 2\pi r dr = \frac{\pi R^4}{8L\mu}\Delta P \qquad (2.3.6)$$

This equation is the famous Hagen-Poiseuille law for Newtonian fluids in laminar flow. [18] If we compare this equation to Darcy's law (equation 2.2.4) the permeability of a single tube yields $\frac{R^2}{8}$.

If the radius, length, injection rate and pressure loss in a capillary tube is known, we can easily use the Hagen-Poiseuille law to calculate the viscosity. To calculate the effective shear rate in the tube equation 2.1.1 and equation 2.3.2 can be combined.

$$\dot\gamma_{eff} = \frac{\tau_w}{\mu} = \frac{R}{2L\mu}\Delta P \qquad (2.3.7)$$

Equation 2.3.5 can be substituted into this equation to create a more simple expression.

$$\dot\gamma_{eff} = \frac{4}{R}V_{avg} \qquad (2.3.8)$$

This equation can also be found by finding $\frac{dV(r)}{dr}$ at r = R. It implies that the shear rate at the wall is the effective shear rate for Newtonian fluids. [17]

For non-Newtonian fluids, the effective viscosity in a tube can be found by using equation 2.3.6. The effective viscosity for a non-Newtonian fluid is defined as the equivalent Newtonian viscosity that results in the same shear stress at a surface at equal volumetric flow rates. This is also how the rheometer operates because the parameter viscosity is defined by the use and definitions of Newtonian fluids. This implies that the effective shear rate for non-Newtonian fluids will be equal to the effective shear rates of Newtonian fluids

of equal effective viscosity to fulfill the definition in equation 2.1.1. Although the wall shear rates in a tube are different whether the fluid is shear thinning or thickening, the only valid effective shear rate for effective viscosities is the effective shear rate for Newtonian fluids. Again, this is because of how viscosity is defined in equation 2.1.4. To show that the volumetric flow rate in a tube is proportional to effective shear rate for both non-Newtonian and Newtonian fluids equation 2.3.6 can be substituted into equation 2.3.8.

$$\dot{\gamma}_{eff} = 4\pi R \cdot Q \qquad\qquad (2.3.9)$$

This can be correlated to the rotational rheometer where the constant injection rate is analogue to the constant rotational speed which is proportional to the shear rate. The pressure loss is analogue to the rotational resistance in the rheometer and is proportional to the viscosity at constant injection rate or shear rate.

If we imagine a non-Newtonian flow through a porous media consisting of thousands of pore channels, the effective viscosity in a single pore channel would depend both on bulk injection rate and on the properties of the fluid, i.e. how the viscosity of the fluid acts upon shear stress. That is, if the bulk injection rate increases or decreases, the distribution of the microscopic flow rate in pore channels will be altered depending on how shear thinning or shear thickening the fluid is. Increasing the bulk injection rate results in a larger increase of microscopic flow rate for small pore channels (lower permeability) compared to larger pore channels (higher permeability) for a shear thinning fluid because the average shear rate in smaller pore channels increases more per unit microscopic flow rate than larger pore channels does. This is due to a smaller cross-sectional flow area. The microscopic average viscosity in smaller pore channels will consequently be smaller resulting in a higher flow rate distribution in smaller pore channels than of a Newtonian fluid of equal initial viscosity. The opposite will happen when the fluid is shear thickening, i.e. increased bulk injection rate results in a higher microscopic flow rate distribution in larger pore channels due to the higher microscopic average viscosity in smaller pore channels. Note that there are other

44

factors affecting the flow, i.e. gravity, slip effects, retention, change of microscopic flow direction, special pore shapes, pore throats etc.

Consequently it is very hard to predict or estimate the local viscosities and shear rates in the porous media in a non-Newtonian flow. Hence, it is possible to calculate apparent viscosity values for non-Newtonian flow in a porous media sample or region, i.e. the average of the effective pore viscosities of all the microscopic pores subjected to the flow. This value can be calculated by using Darcy's law at steady state injection (equation 2.2.4). However, due to possible retention of polymers (the non-Newtonian fluid) causing decreasing permeability, it is better to compare the pressure loss to a Newtonian injection afterwards at equal injection rate and assuming constant rock properties. Using Darcy's law directly might cause false apparent viscosity calculations due to the change of permeability (retention). [17]

$$\frac{\mu_{app}}{\mu_N} = \frac{\frac{k \cdot A}{Q \cdot L} \Delta P_{n-N}}{\frac{k \cdot A}{Q \cdot L} \Delta P_N} = \frac{\Delta P_{n-N}}{\Delta P_N}$$

$$\rightarrow \mu_{app} = \frac{\Delta P_{n.-N}}{\Delta P_N} \cdot \mu_N \qquad\qquad (2.3.10)$$

This apparent viscosity is often called the resistant factor, RF, for the particular fluid.

To estimate the apparent shear rate in a porous media we also need to know the total pore wall area subjected to flow and the total frictional force. It is impossible to estimate this exact area, due to different pore shapes and pore sizes. From equation 2.3.8 in a capillary tube we know that the effective shear rate depends on the average velocity and radius. The can be extrapolated to a porous medium where V_{avg} is the average pore velocity and R is the average pore radius. The Dupit-Forsheimer assumption relates the average pore velocity to bulk measurements [17];

$$V_{p,avg} = \frac{V_{bulk}}{\varphi} = \frac{Q_{bulk}}{A_{bulk} \cdot \varphi} \qquad (2.3.11)$$

The average pore radius can be expressed by permeability, porosity and a factor *C* depending on the pore geometry. [19]

$$R_{p,avg} = \sqrt{\frac{8kC}{\varphi}} \qquad (2.3.12)$$

Equation 2.3.11 and 2.3.12 can be substituted into equation 2.3.8 to create an expression for apparent shear rate in porous media based on bulk injection velocity, permeability, porosity and a pore geometry factor. [17]

$$\dot{\gamma}_{app} = \alpha \frac{4u}{\sqrt{8\varphi k}} \qquad (2.3.13)$$

α is the pore geometry factor and u is the bulk injection velocity. The advantage of using this formula instead of a single proportionality factor between apparent shear rate and injection rate is that different values of α can be compared or assumed for porous media with varying porosity and permeability. This relationship is useful and valid for both Newtonian fluids and non-Newtonian fluids. Equation 2.3.13 is used in the experimental calculations.

2.3.6 Viscoelastic Effects in Porous Media

The viscoelastic effect is the shear thickening region, i.e. the region where the resistance factor increases per unit injection rate. In rheometer measurements, this region appears when the shear forces begin to stretch the fluid molecules. In a porous media this effect behaves differently. It is reasonable to assume that even at very low injection rates fluid molecules are being stretched in small pore channels. However, the shear thickening effect does not become evident before the transit time between pore throats is higher than the relaxation time of the fluid molecules. When the molecules do not have enough time to return to their original configuration after being stretched in a small pore channel, the molecules stays stretched which increases its resistance to stretch further yielding in a higher resistance factor. If the transit time (which is proportional to injection rate) continues to increase so will the resistance factor. When mechanical degradation occurs (breaking of molecules) the resistant factor will decrease. [17] [11]

3 Experimental Set-Up and Procedure

The idea behind the experiments in this thesis was to first prepare ten different concentrations of HPAM 3630S and 3230S, followed by tests using the rheometer. The information needed from the rheometer was viscosity at different shear rates. Each polymer concentration was tested at least twice to make sure no large deviations in the results were present. The final results from the rheometer were also compared to earlier results. The next step was to inject two different concentrations of each HPAM polymer into two cores in series, while measuring the differential pressure over each core sample at different injection rates. Since injection rate is proportional to shear rate, we can calculate the apparent viscosity of the polymer in the porous media at different injection rates. This injection rate dependent viscosity can be compared to the rheometer results from the same polymer concentration. Water permeability was measured before and after polymer injections. The effluent polymer solutions at low and high injection rates were collected and brought to the rheometer for new tests.

Polymer concentrations used for rheometer testing:

HPAM 3630S and HPAM 3230S: 100ppm, 200ppm, 400ppm, 600ppm, 800ppm, 1000ppm, 1500ppm, 2000ppm, 3000ppm, 5000ppm

The polymer solutions were all made with brine consisting of 6g NaCl and 1g NaHCO^3 per liter distilled water.

Polymer concentrations used for injection:

HPAM 3630S: 800ppm and 2000ppm

HPAM 3230S: 1500ppm and 3000ppm

1500ppm and 3000ppm is chosen for 3230S injections because they are the closest behaving polymer concentrations in rheology measurements when compared to HPAM 3630S 800ppm and 2000ppm. This makes it possible to compare if the rheology of HPAM 3230S behaves differently than the rheology of HPAM 3630S in porous media.

With these experiments, it is possible to show how the viscosity of the polymer solutions varies with injection rate compared to shear rate in a rheometer, the difference in the water permeability of the core samples before and after polymer injections and the difference in the rheology of polymer solutions before and after porous media injections at high and low rates.

3.1 Procedure

The experiments were performed in this order:

1. Prepare a stock solution of 0,5L 5000ppm HPAM 3630S

2. Prepare diluted solutions of the HPAM 3630S stock solution at following concentrations; 100ppm, 200ppm, 400ppm, 600ppm, 800ppm, 1000ppm, 1500ppm, 2000ppm, 3000ppm

3. Run two individual samples of every concentration, including the 5000ppm solution, on the rheometer.

4. Prepare two Bentheimer sandstone core samples and measure length and diameter. Mount the core samples in two separate core holders with a sufficient confining pressure, usually between 20 and 30 bars.

5. Apply a vacuum to both cores by using a vacuum pump.

6. Saturate both cores with brine by using a pump. The cumulative volume of brine injected can be considered the effective pore volume.

7. Connect the two core holders in series and connect them to a pump, a backpressure regulator and two differential pressure gauges over each core holder. Make sure to fill all the lines with brine and avoid any air in the system. See fig. 1.1.

8. Inject brine through both cores at different injection rates. Always let the differential pressures stabilize before moving to the next injection rate. Use Darcy's law and the differential pressures at given injection rates to calculate the permeability of each core sample.

9. Prepare a slave cylinder filled with a fresh batch of 800ppm 3630S and connect it to the pump. Avoid any air in the slave cylinder.

10. Inject the polymer solution into the core samples at decreasing injection rates. Can be a smart idea to start at a midrange injection rate and increase accordingly until the maximum range of the pressure gauges have been reached. Then start the actual decreasing injection at minimum ten different injection rates. Remember to wait for a steady flow, i.e. stable differential pressure before every measurement.

11. Take an effluent sample of the polymer at the very lowest injection rate. Remember to catch the sample after at least injecting 1 PV of polymers at the given injection rate.

12. Disconnect the slave cylinder and measure water permeability as described in 8.

13. Reconnect the slave cylinder filled with HPAM 3630S 800ppm and inject the polymer with an increasing injection rate using the same rates as in 10. Remember to wait for a steady flow, i.e. stable differential pressures before every measurement.

14. Take a new effluent sample at the highest injection rate. Again, remember to flood the cores with at least 1 PV of polymers at the given injection rate before catching the sample.

15. Again, disconnect the slave cylinder and measure water permeability as described in 8.

16. Repeat step 10-15 with a fresh batch of 2000ppm 3630S using the same core samples.

17. Finally, repeat all of the steps above using HPAM 3230S using two new unused Bentheimer core samples. HPAM 3230S 1500ppm will replace HPAM 3630S 800ppm, and HPAM 3230S 3000ppm will replace HPAM 3630S 2000ppm.

3.2 Experimental Set-Up

3.2.1 Preparation of Polymer Solutions

All of the polymer solutions were diluted from a stock solution of 5000ppm. The stock solution is made from brine and polymer powder using a magnetic stirrer.

$$5000ppm = \frac{5g\ polymer}{1000g\ brine} = \frac{2,5g\ polymer}{500g\ brine} \tag{3.2.1}$$

The dry polymer powder has an active percentage of about 90. That is, we have to add about 10% extra dry polymers to the brine.

$$\frac{2,5g}{0,9} \approx 2,78g$$

This implies usage of 2,78g dry polymer powder per 500g of brine solution to make a stock solution of 5000ppm. The procedure is rather simple;

- Fill a suitable open glass container with 500g of brine.
- Drop a suitable magnet (shear friendly) into the container
- Use a magnetic stirrer to create a vortex almost reaching the bottom of the container
- Carefully sprinkle ≈ 2,78g of polymer powder into the wall of the vortex, not the bottom.
- Wait about ten minutes until the vortex has disappeared
- Turn the magnetic stirrer down to the lowest, yet smooth turning level.
- Wait another 24 hours or so and the stock solution is ready to use.

The stock solution was diluted when lower concentrations were made, using the magnetic stirrer at low speeds due to possible mechanical degradation.

Polymer solutions are sensitive to light and high temperatures, so all of the polymer solutions were kept in a fridge throughout the experiment. Solutions older than a couple of weeks, especially lower concentrations, were disposed and replaced by a freshly made solution.

3.2.2 Chemicals

Presented is a table of chemicals used in the experiments.

Table 1: List of chemicals used the experimental work.

Chemical	Manufacturer/Ingredients
Sodium Hydrogen Carbonate (NaHO$_3$)	Fluka
Sodium Chloride (NaCl)	Sigma-Aldrich
FLOPAAM 3630 S	SNF Floerger
FLOPAAM 3230 S	SNF Floerger
Brine	6g NaCl, 1g NaHO$_3$ /1L H$_2$O

3.2.2 Rheometer

The rheometer sequences were programmed by researcher Tormod Skauge. The shear rate was set to run from $0.01s^{-1}$ to $5000s^{-1}$ and the temperature was set at 22°C. Cone and plate geometry was used throughout the experiments. The spindle that was used had a 4 degree angle, 40mm diameter and a truncated cone. Loading samples is very well described in the rheometer software, the important part is to be accurate on loading the correct volume of the sample and clean the geometry and spindle thoroughly after each run.

3.2.3 Polymer injections and permeability measurements
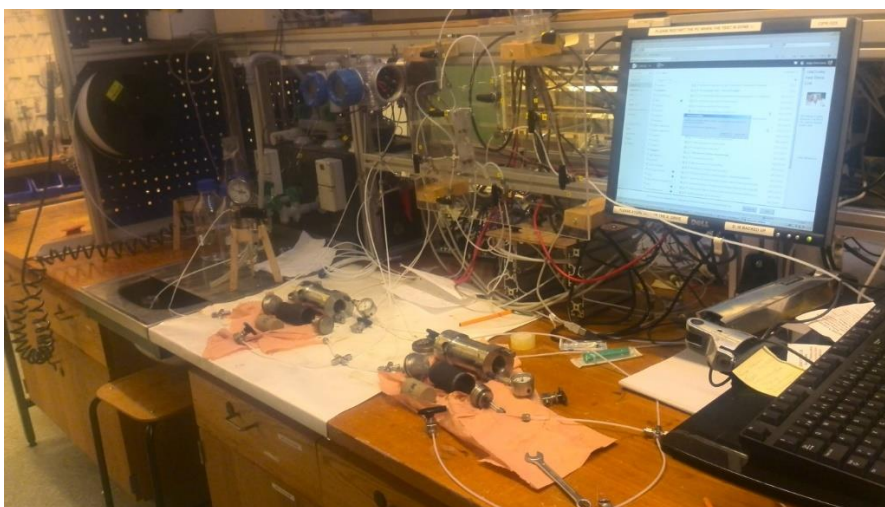
Figure 20: Picture of the experimental set-up for core injections.

This picture shows the actual set-up in the laboratory. The pump and differential pressure gauges were connected to the computer for monitoring and control. During permeability measurements the pump was connected directly to the inlet of the first core, of course using brine in the pump reservoir. During polymer injections, spring water was used in the pump reservoir and a 1000mL slave cylinder was used to displace the polymers. As mentioned, the entire fluid system from the pump reservoir to the outlet must be air free. Also, be aware of sufficient confining pressure in the core holders at all times to prevent leaks, should read at least 20 bars. A backpressure regulator was used at the outlet to keep the fluids in the tubing from escaping due to gravity. It was set at around 10 bars.
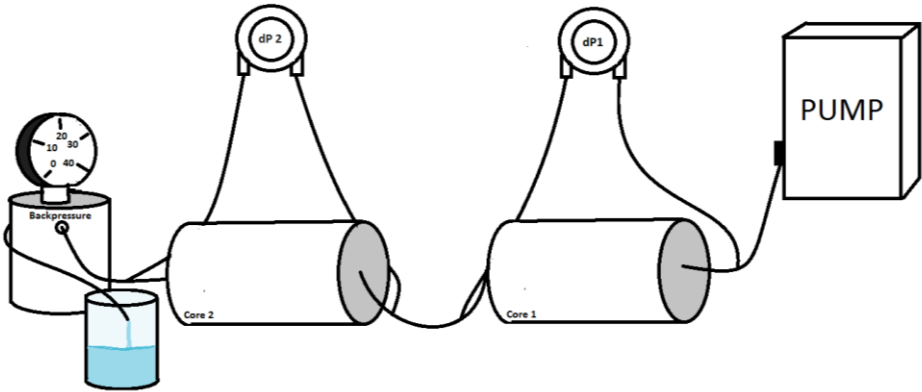
Figure 21: Basic illustration of the experimental set-up.

This figure shows a clearer sketch of the basic elements of the core injection set-up.

3.3 Equipment

Table 2: Equipment utilized in the experimental work.

Equipment	Manufacturer	Model	Properties	Uncertainty
Pump	Quizix	QL-700	Maximum rate; 10ml/min	0.01%
Differential Pressure Transmitter, dP1	Fuji Electric	FCX-series	Max Range; 1300mBar	1% of set range
Differential Pressure Transmitter dP2,	Fuji Electric	FCX-series	Max Range; 5000mBar	1% of set range
Rheometer	Malvern	Kinexus Pro	Rotational. Torque range; 2nNm to 200mNm	5%
Spindle	Malvern	CP 4/40 SP1459 SS	Angle; 4° Diameter; 40mm	-
Backpressure regulator	MI	-	-	-
Valves, fittings	Swagelok	-	-	-
PFA tubing	Teknolab	-	Inner diameter; 1.6mm	-

3.4 Sources of Error

There are a lot of variables in a larger experiment over time. Uncertainty is a statistical property, the probability of accuracy. It is very difficult to predict how accurate test results are when so many factors play a role. The rheometer results are stated to have an uncertainty of 5% depending on the geometry and fluid properties. The core injections depend on a lot more variables, both equipment based and human error based. The uncertainty of the pressure loss and injection rate combined is believed to be at least 5%.

4 Results and Discussion

All tables and data from the experiments can be found in appendix.

4.1 Assumptions

In these experiments following assumptions were made:

- The porosity in the cores was left unchanged during polymer injections
- The permeability changed immediately when the polymer flood entered the core
- Brine viscosity is 1cP
- Gravity was neglected
- Pressure affecting the viscosity was neglected
- Temperature affecting viscosity during porous media injections was neglected, temperature was assumed to be 22°C at all times
- The pore geometry constant α (equation 2.3.13) is constant for each core sample throughout the experiments

4.2 HPAM 3630S

4.2.1 Rheology measurements

As previously mentioned, two samples of each of the concentrations 100ppm, 200ppm, 400ppm, 600ppm, 800ppm, 1000ppm, 1500ppm, 2000ppm, 3000ppm and 5000ppm were measured using the rheometer. The tables containing these rheology results can be found in Appendix A.
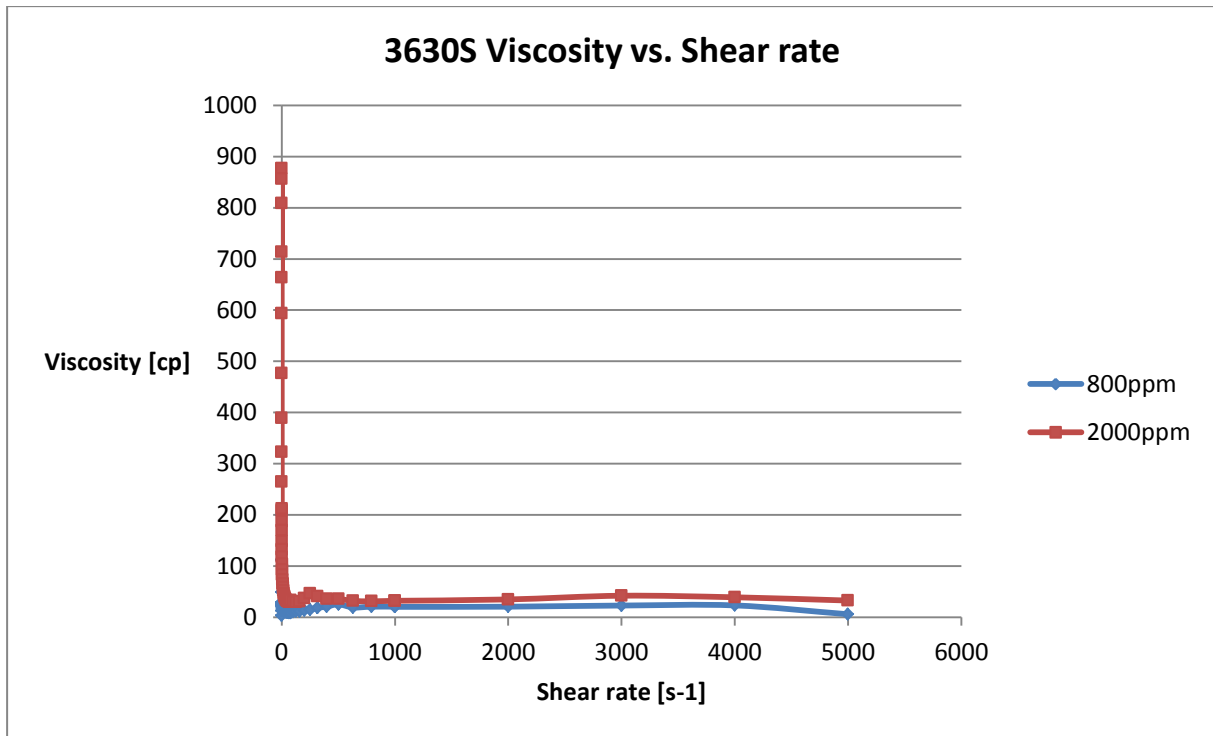
Figure 22: Viscosity curves for 800ppm and 2000ppm HPAM 3630S.

In figure 22 the rheometer results from 800ppm and 2000ppm 3630S has been plotted in a regular plot. We immediately see that the viscosity is dropping at very low shear rates and that the curve does not give us any valuable insight to the rheology properties. A better way to display these data would be using a log-log plot.
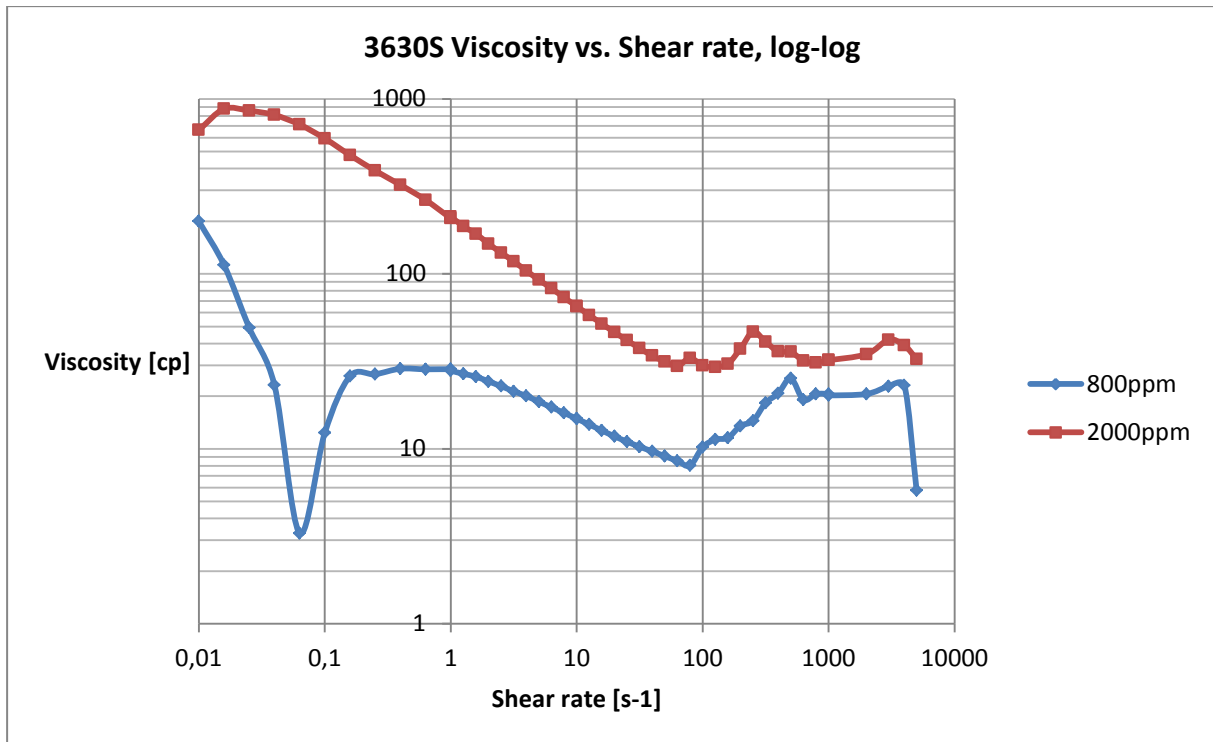
Figure 23: Viscosity log-log curves for 800ppm and 2000ppm HPAM 3630S.

In this log-log plot, we can more clearly see how the viscosity varies with shear rate. Using this plot we can also spot some weaknesses in the rheometer measurements. There are a lot of variations, or noise, at the very smallest and largest shear rates. For 800ppm I would say that every viscosity measurement at a smaller shear rate than $0.4s^{-1}$ should be disregarded because the readings should begin at a Newtonian plateau or during shear thinning. The viscosity measurements after the highest reading during shear thickening should also be disregarded due to turbulence or loss of fluid. At higher concentrations the noisy regions at low shear rates tend to get a lot smaller due to more friction which gives more stable readings. The more viscoelastic fluids tends to have more unstable readings at high shear rates, most likely due to the rod climbing (Weissenberg) effect (figure 5). The unstable regions have been edited out in the rest of the plots and in the tables in appendix.
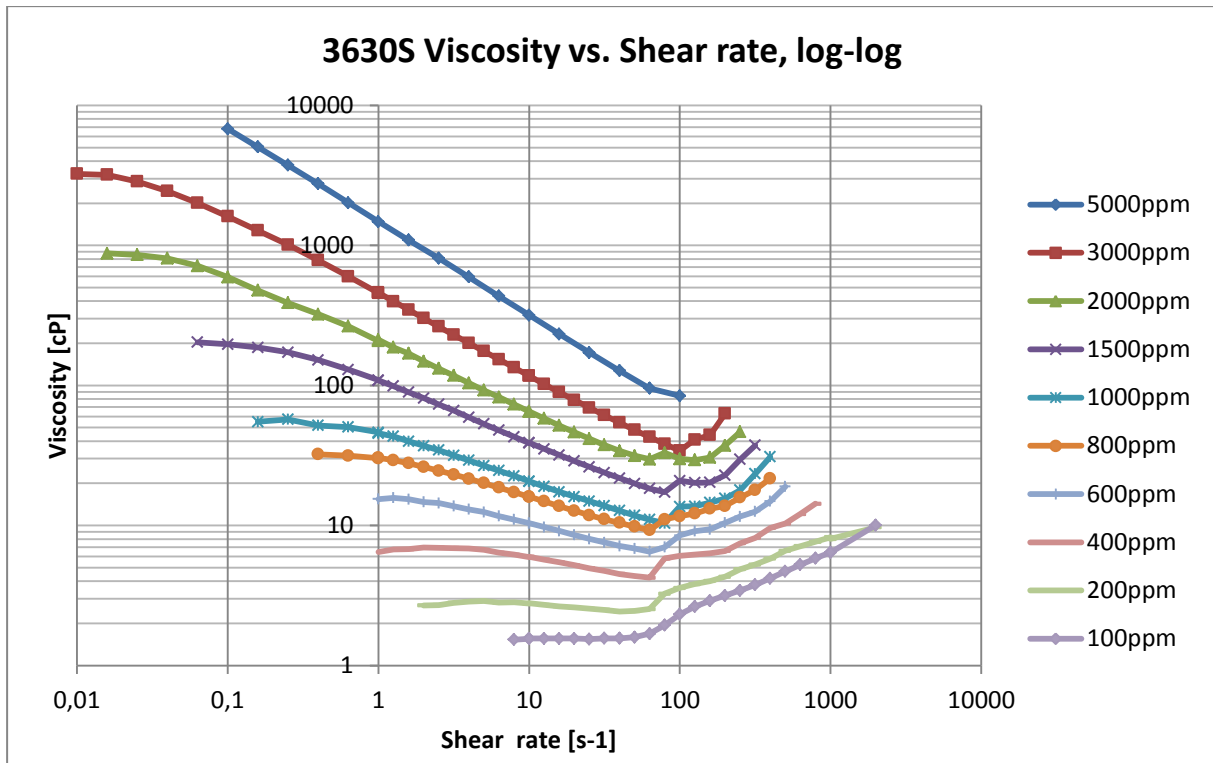
Figure 24: Viscosity log-log curves for all ten concentrations of HPAM 3630S.

The rheometer results for HPAM 3630S displayed in figure 24 shows behavior according to previous literature. [17] A short Newtonian plateau is seen at lower concentrations as well as a less steep shear thinning region. This makes sense because there are less polymer molecules per test sample i.e. more water like behavior. A Newtonian plateau and a large shear thickening region is not seen in the solutions of high concentration due to limitations in the cone and plate geometry. It can be expected that the higher concentrations would show a steeper shear thickening effect due to its more viscoelastic properties.

4.2.2 Core Data

The two cores in the 3630S core flooding were named HF 1 and HF 2.

Table 3: Core data for HPAM 3630S injections.

Differential Pressure Gauge	dP2	dP1
Bentheimer Sandstone	Core HF 2	Core HF 1
Diameter [cm]:	3.76	3.74
Length [cm]:	5.84	5.63
Cross-sectional Area [cm^2]	11.10	10.99
Pore Volume [mL]:	14.8	15.2
Porosity	0.24	0.26
Permeability Before Polymer Injection [mD]	1734	1963
Pore Geometry Constant α (picked)	5	3

The constant α for HF 1 has been set to 3 and HF 2 has been set to 5 throughout the calculations of the resistant factor. This is because the shear thickening zones in the porous media coincides with the rheometer results. The reason is simply just to make the results comparative. The onset of shear thickening might happen at a lower or higher shear rate, yielding in a different value of α.

The absolute permeability was calculated with Darcy's law (2.2.4) using a linear trend line (dQ/dP) through the measured differential pressure values on a Q vs. dP plot. It was measured by injecting brine.

$$k = \frac{dQ}{dP} \cdot \frac{\mu \cdot L}{A}$$

(4.2.1)

4.2.3 800ppm 3630S Injection
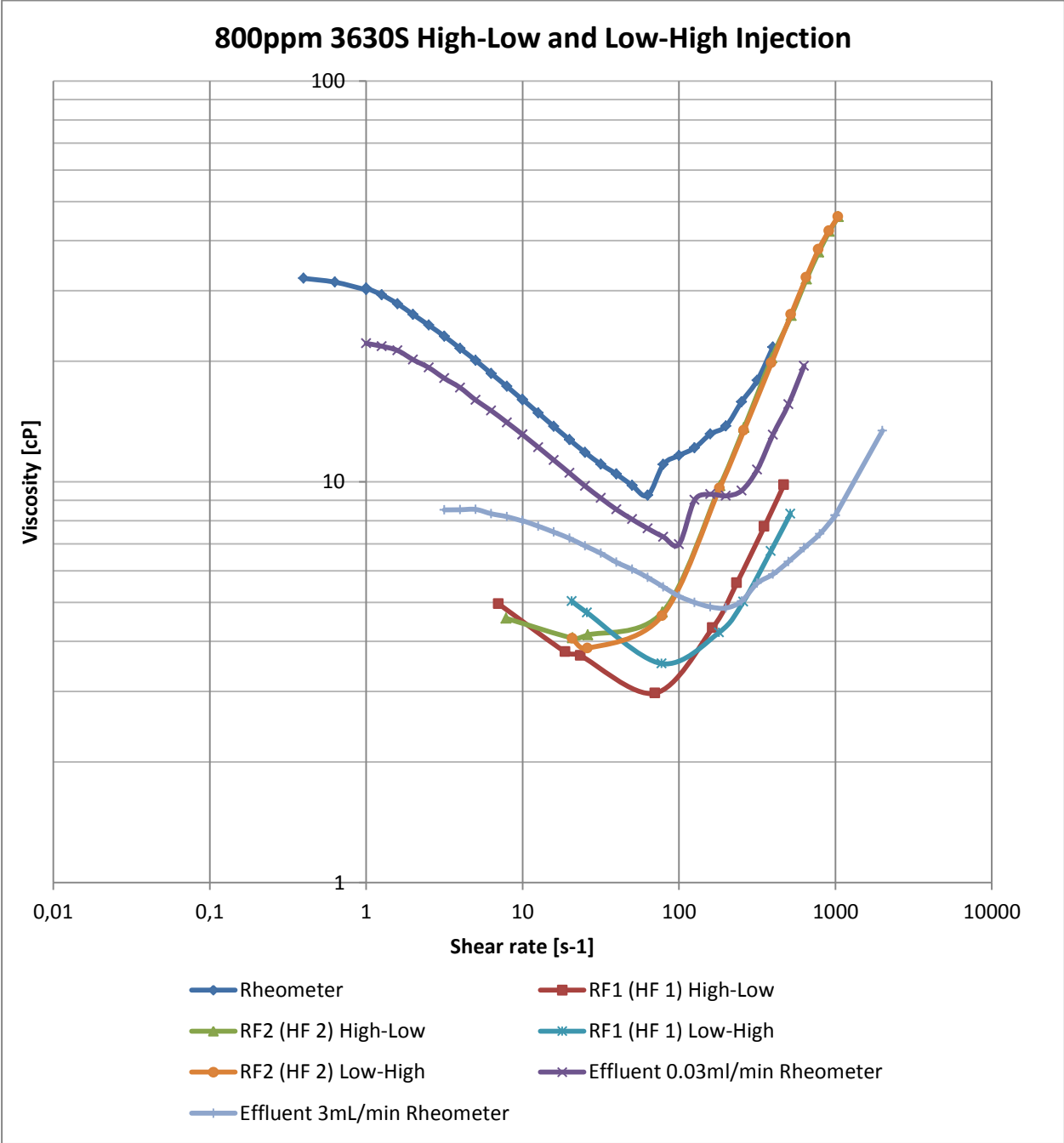
Figure 25: Viscosity log-log curves for porous media injections, effluent samples and original rheometer data for HPAM 3630S 800ppm.

4.2.4 2000ppm 3630S Injection
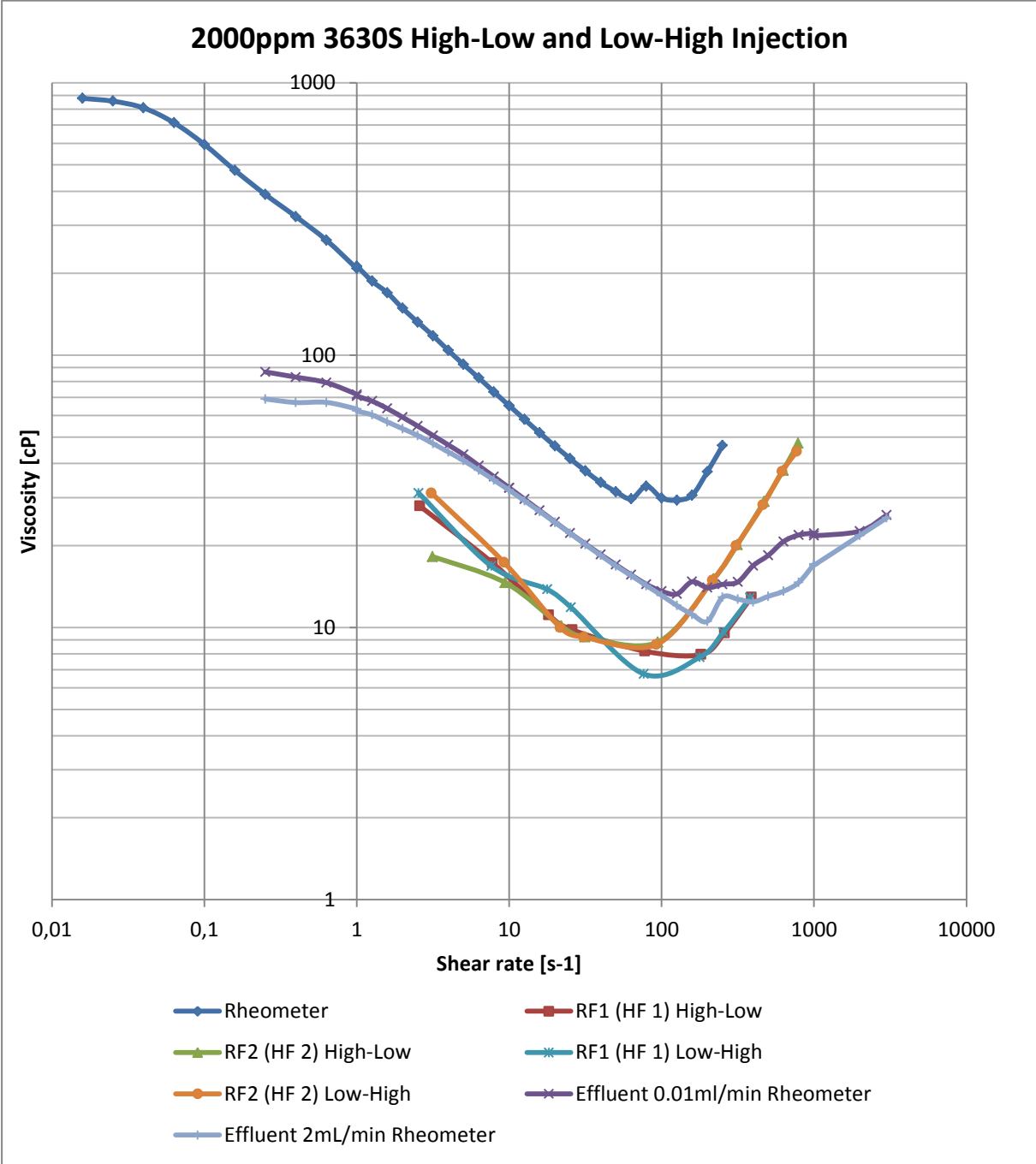
Figure 26: Viscosity log-log curves for porous media injections, effluent samples and original rheometer data for HPAM 3630S 2000ppm.

4.2.5 Permeability Effect of HPAM 3630S Injections
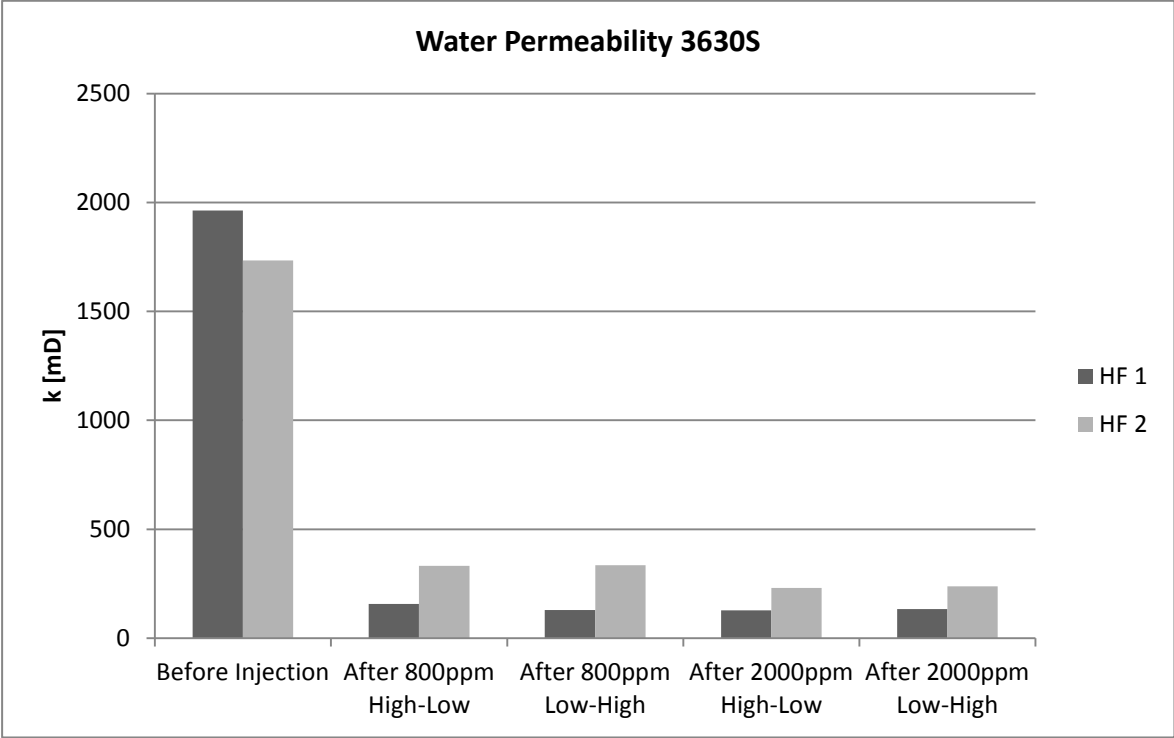
Figure 27: Absolute permeability measurements throughout the experiments with HPAM 3630S.

The permeability measurements after each polymer injection show that the big alternation of the rocks permeability happens during the very first flow of polymers through the core. The following measurements show very small changes in rock permeability. Consequently, most of the polymer retention should happen during the first pore volumes injected.

4.3 HPAM 3230S

4.3.1 Rheology Measurements

The same concentrations as measured with 3630S were measured using HPAM 3230S. Rheometer programming was also identical. All tables containing data from 3230S rheometer results can be found in Appendix B.
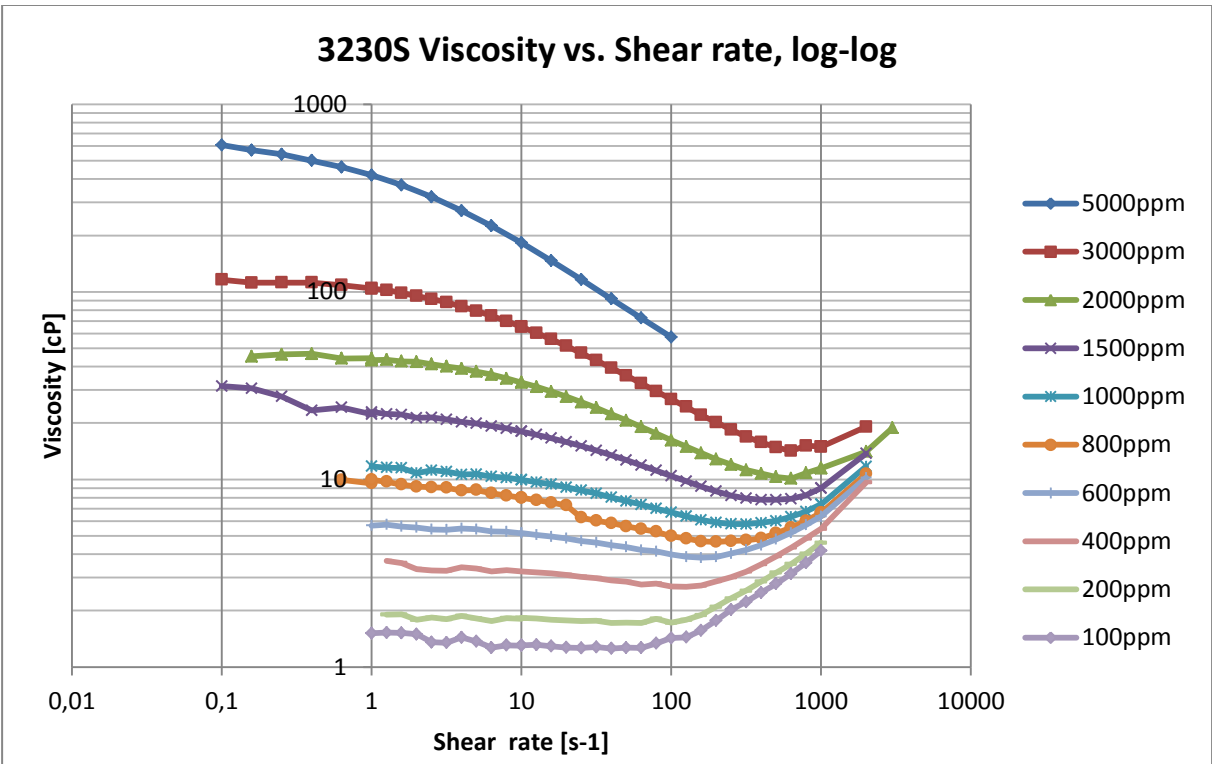
Figure 28: Viscosity log-log curves for all ten concentrations of HPAM 3230S.

If we compare this plot to figure 24, it is quite obvious that 3230S has lower viscosities at all concentrations. The degree of shear thinning and shear thickening in the curves also seems to be smaller. HPAM 3230S does have smaller chain molecules, which results in less shear thinning properties and less viscoelastic properties, thus less shear thickening. The choice of rheometer geometry probably also play an effect on both polymers because the shear thickening region probably exceeds beyond the last stable reading. The concentrations for 3230S core injections were chosen after all of the 3630S and 3230S rheology measurements were performed. The goal was to have two concentrations that had a similar viscosity at a

64

shear rate of 10s^{-1} compared to HPAM 3630S 800ppm and 2000ppm. . This shear rate was picked because it is well placed in the middle of the noise-free rheometer results.
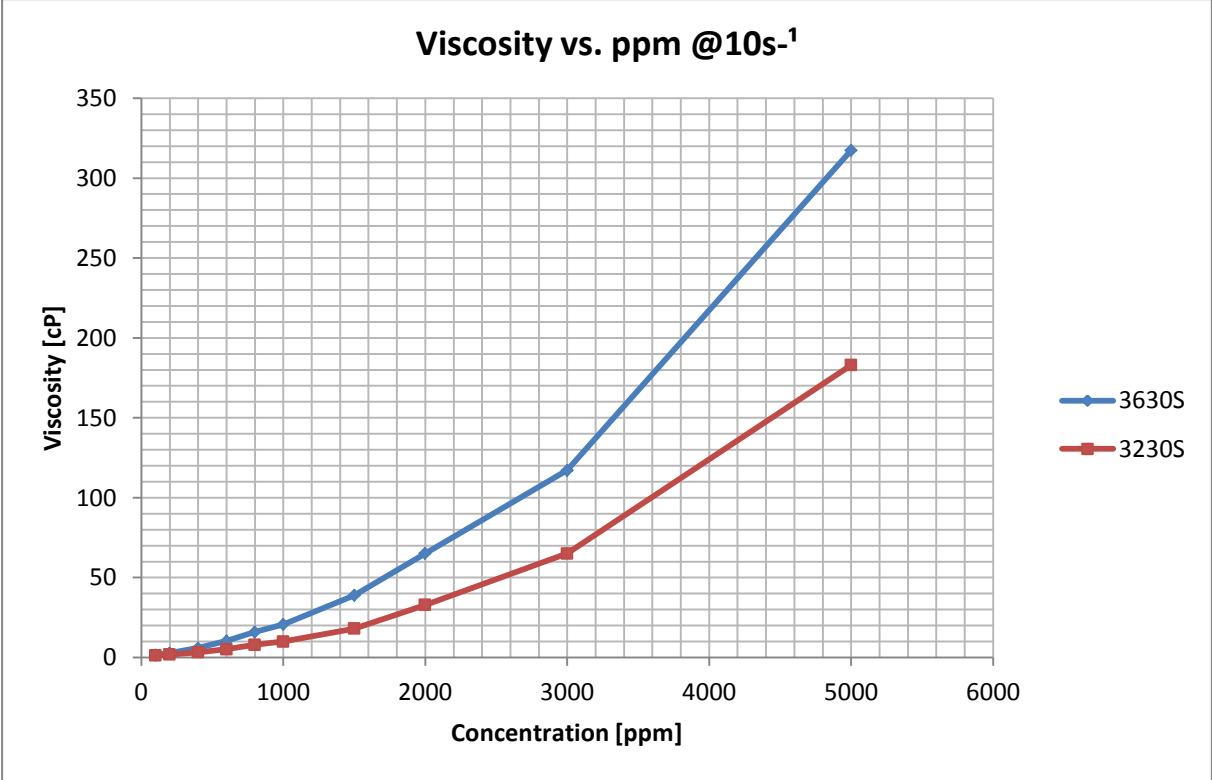
Figure 29: Viscosity curve for different concentrations of HPAM 3630S and HPAM 3230S at shear rate 10s^{-1}.

From this plot we see that 3630S 2000ppm have a similar viscosity as 3230S 3000ppm. We also see that 3630S 800ppm have a similar viscosity as 3230S 1500ppm. Therefore, HPAM 3230S 1500ppm and 3000ppm were chosen for polymer injections.
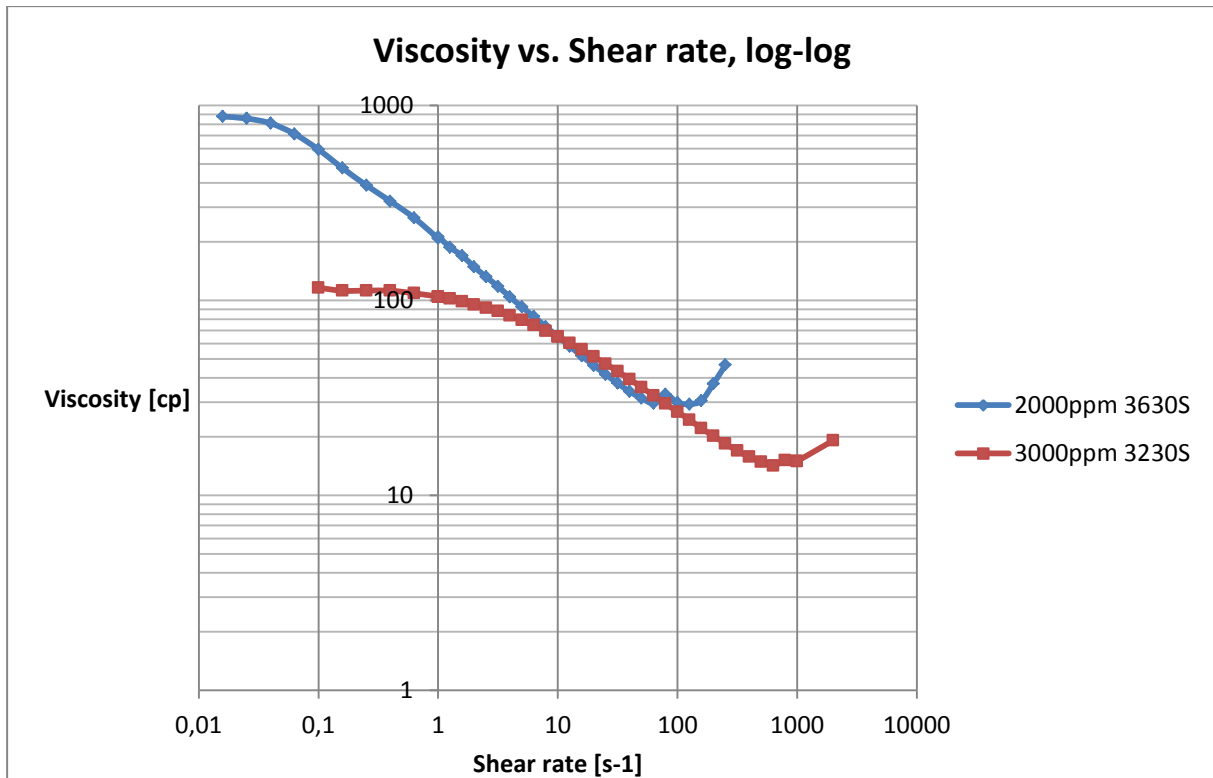
Figure 30: Viscosity log-log curves for HPAM 3630S 2000ppm and HPAM 3230S 3000ppm.

This plot shows how different the two polymers with equal viscosity at $10s^{-1}$ behave at different shear rates. It is obvious that the lower molecular weight 3230S have a smaller initial viscosity, a shorter shear thinning region and show shear thickening at higher shear rates than the 2000ppm 3630S. Also, it is important to notice that the shear thinning curvature is less steep for 3230S.
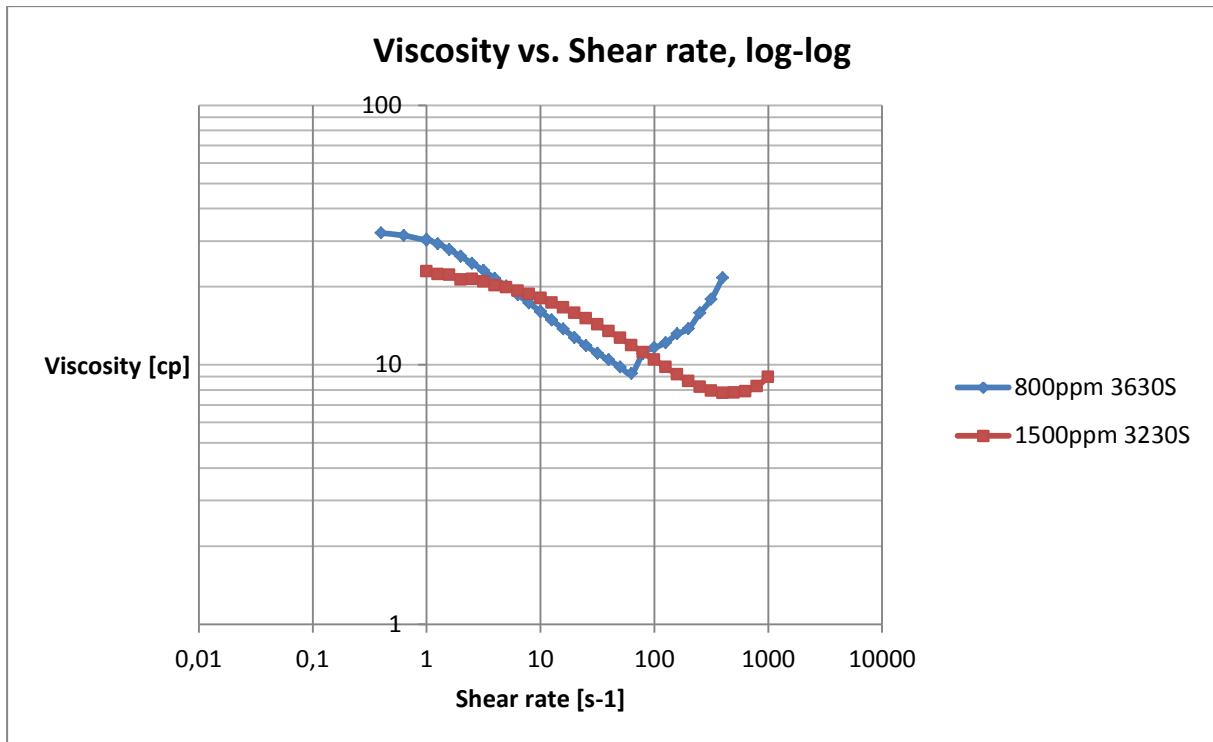
Figure 31: Viscosity log-log curves for HPAM 3630S 800ppm and HPAM 3230S 1500ppm.

The rheometer results for 3630S 800ppm and 3230S 1500ppm also show similar differences in behavior. The onset of shear thickening seems to start at a higher shear rate compared with 3630S. This is probably due to less viscoelastic properties. HPAM 3630S seem to have sharper definitions between the rheological regions and HPAM 3230S has the more smooth curvature. The degree of shear thinning also seems to be higher for 3630S.

4.3.2 Core Data

The two cores in the 3230S core flooding was named HF A and HF B.

Table 4: Core data for HPAM 3230S injections.

Differential Pressure Gauge	dP2	dP1
Bentheimer Sandstone	**Core HF B**	**Core HF A**
Diameter [cm]:	3.77	3.76
Length [cm]:	5.57	5.55
Cross-Sectional Area [cm^2]	11.16	11.10
Porevolume [mL]:	14.9	15.2
Porosity	0.24	0.25
Permeability Before Polymer Injection [mD]	1373	1922
Pore Geometry Constant α (picked)	5	5

The constant α for HF A has been set to 5 and HF B has been set to 5 throughout the calculations of the resistant factor. This is because the shear thickening zones in the porous media coincides with the rheometer results. The reason is simply just to make the results comparative. The onset of shear thickening might happen at a lower or higher shear rate, yielding in a different value of α.

The absolute permeability was calculated using equation 4.2.1.

4.3.3 1500ppm 3230S Injection
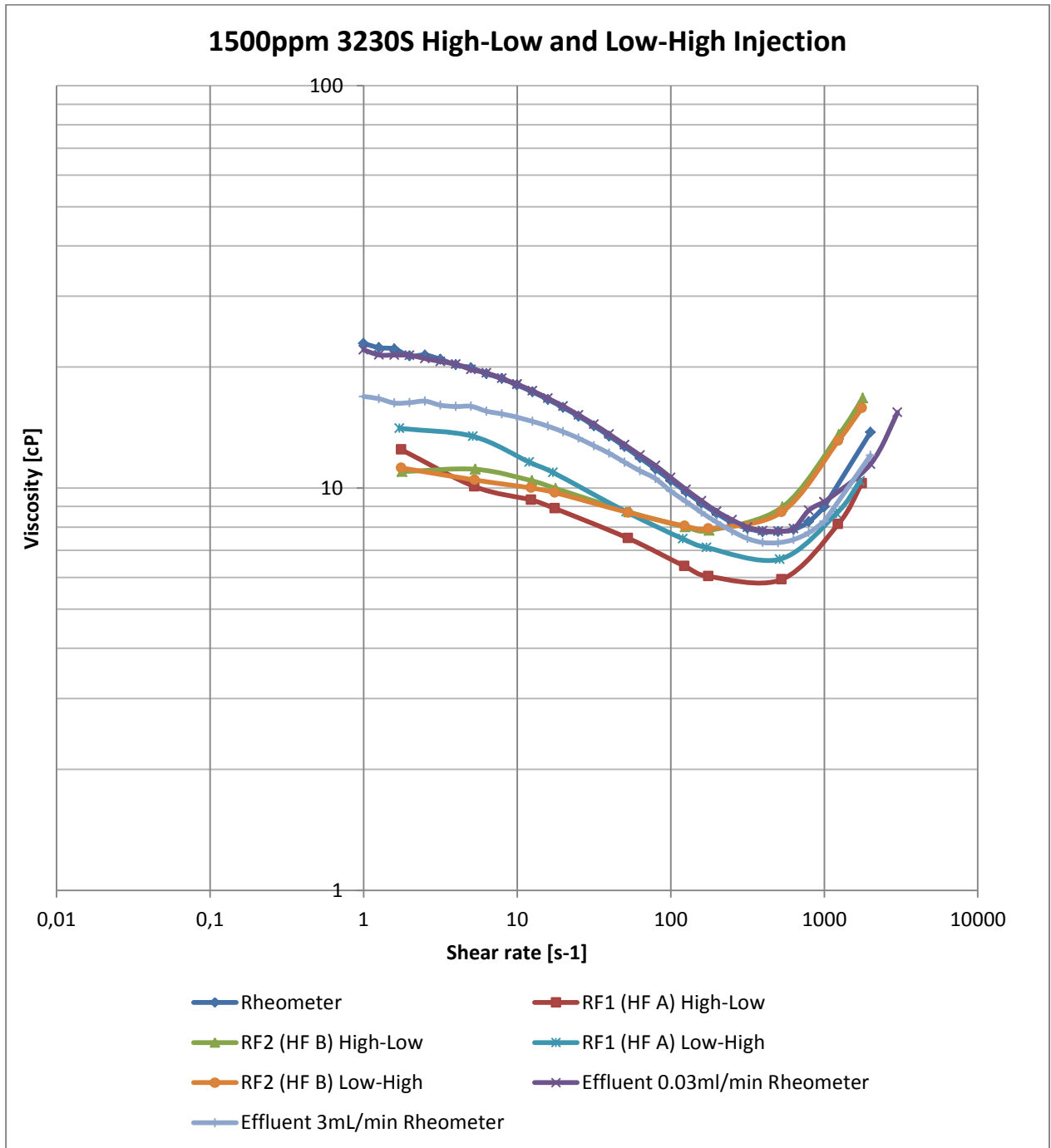
Figure 32: Viscosity log-log curves for porous media injections, effluent samples and original rheometer data for HPAM 3230S 1500ppm.

4.3.4 3000ppm 3230S Injection
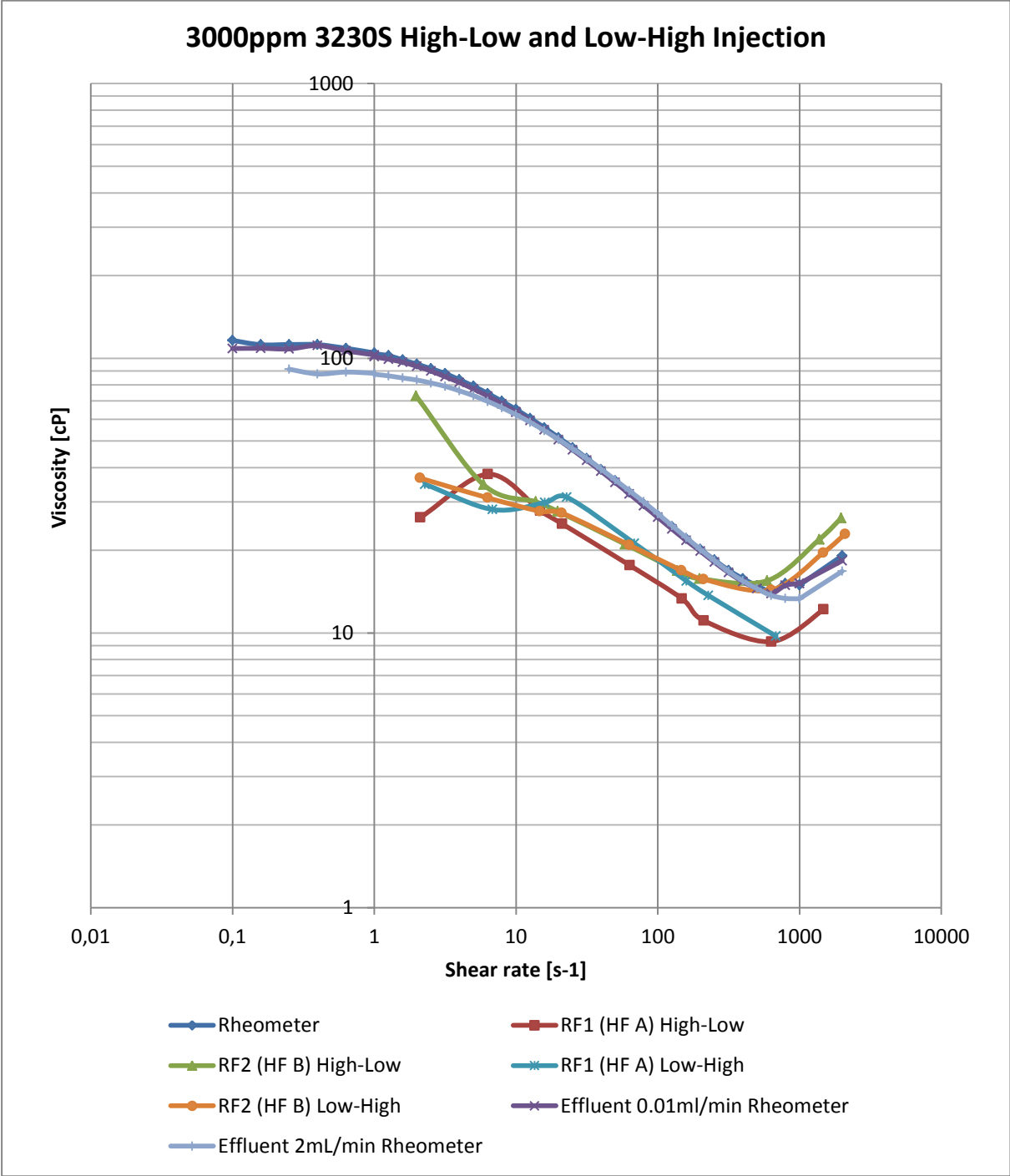
Figure 33: Viscosity log-log curves for porous media injections, effluent samples and original rheometer data for HPAM 3230S 3000ppm.

4.3.5 Permeability Effect of HPAM 3230S Injections
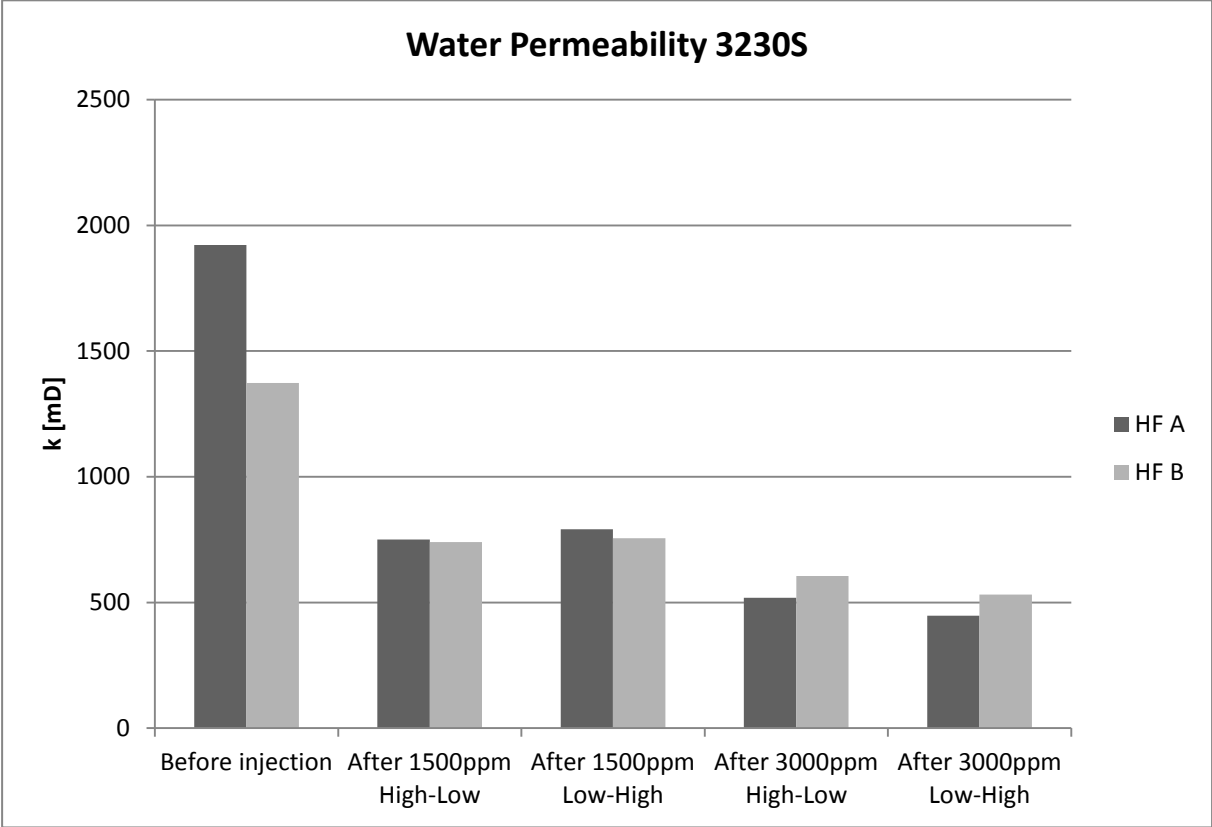
Figure 34: Absolute permeability measurements throughout the experiments with HPAM 3230S.

The reduction in permeability is not as evident after HPAM 3230S as after injection of HPAM 3630S. The reduction is however somewhat stable after the larger reduction after the very first injection of polymers.

4.4 In-Situ Comparison between HPAM 3630S and HPAM 3230S
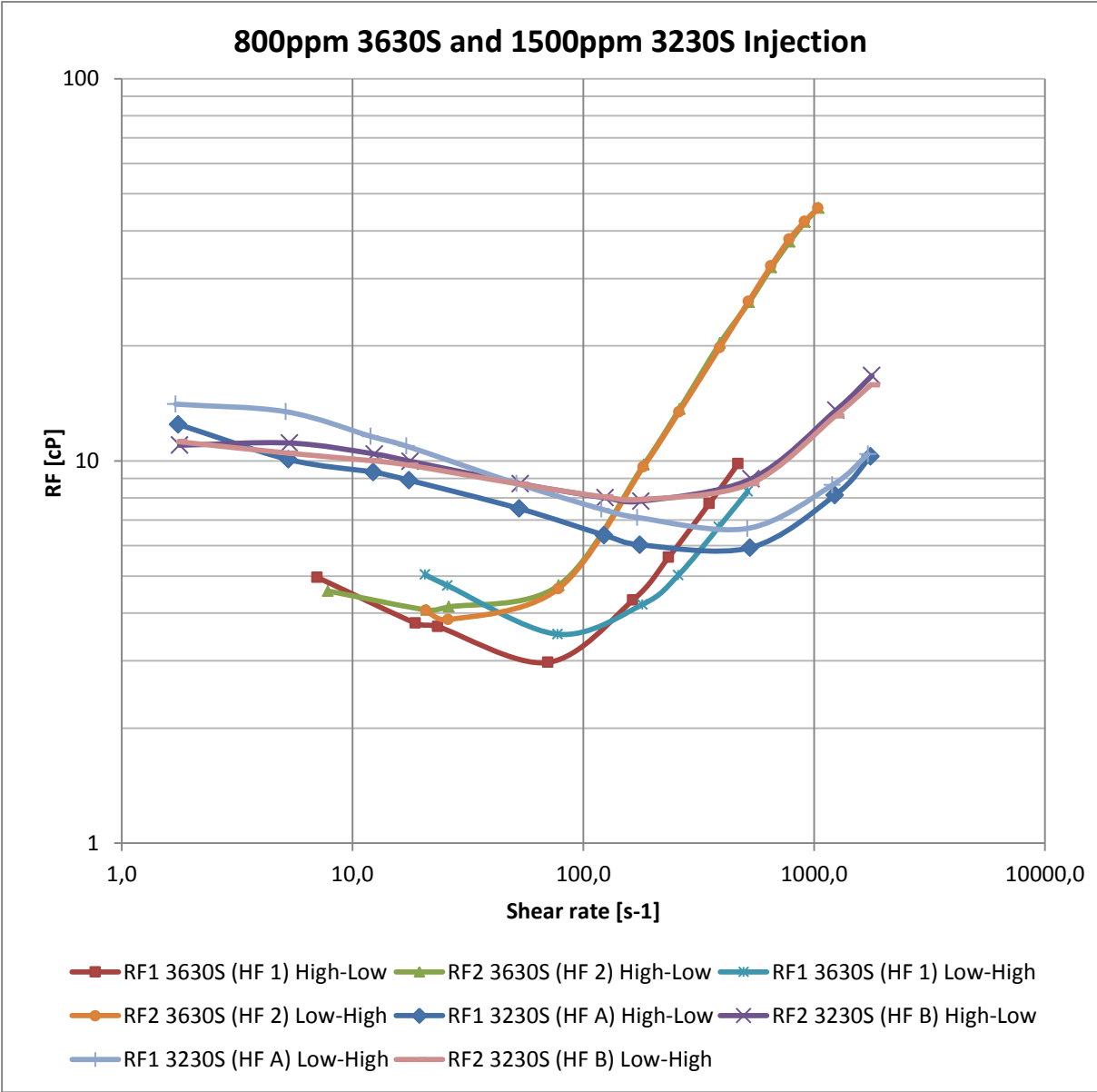
Figure 35: In-situ viscosity log-log curves for HPAM 3630S 800ppm and HPAM 3230S 1500ppm.
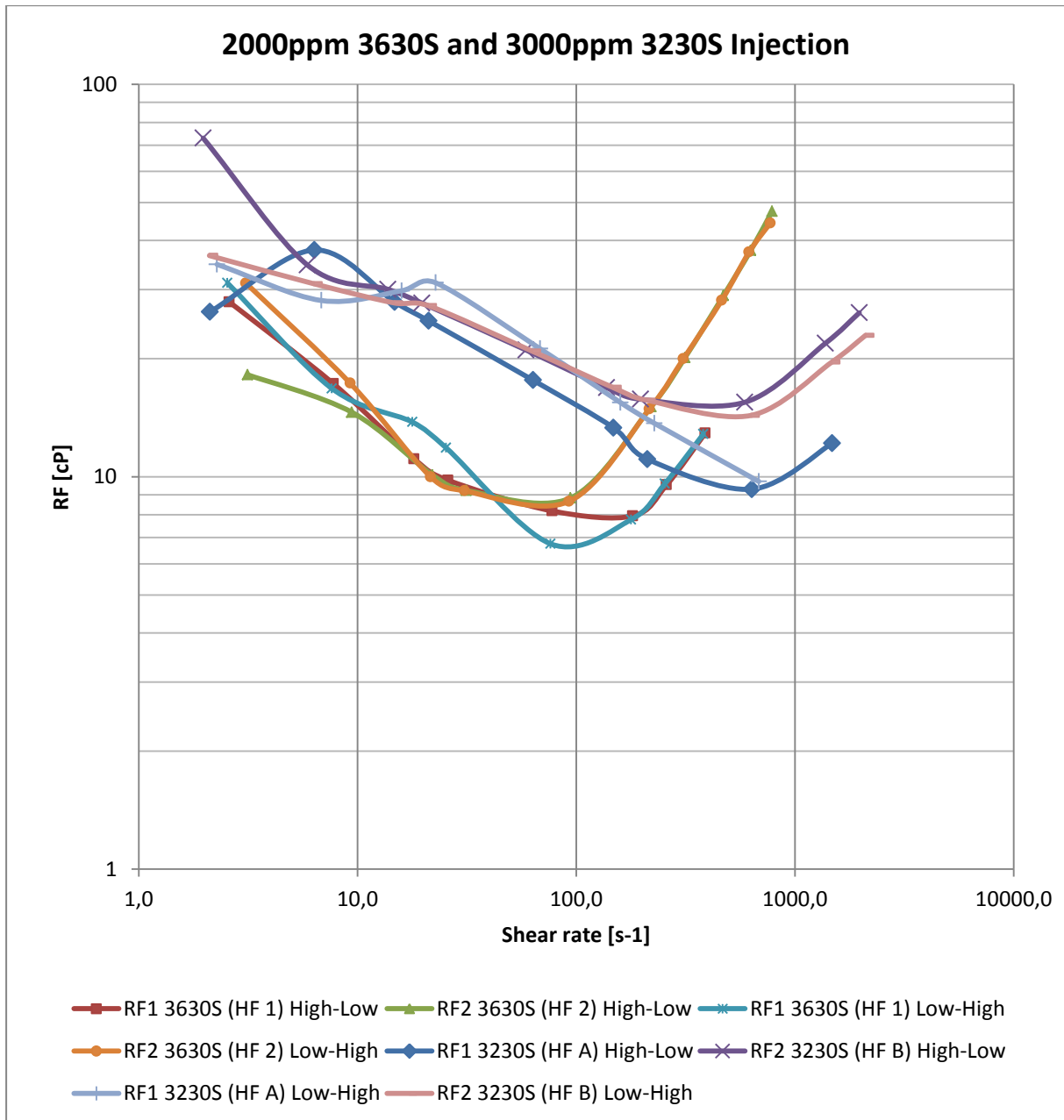
Figure 36: In-situ viscosity log-log curves for HPAM 3630S 2000ppm and HPAM 3230S 3000ppm.

4.5 Discussion of Injection Data

There are no larger signs of deviation in core HF 2 and HF B when it comes to whether the injection rate starts descending or rising. However, in core HF 1 and HF A at 800ppm 3630S injection the resistant factor seems to be higher at higher apparent shear rates when the injection starts at maximum injection rate. This difference seems to be due to different permeabilities after each injection. The resistant factor at medium to low injection rates for 3630S 800ppm and 3230S 1500ppm through the first core seems to be higher when the injection starts at the minimum injection rate. This might be due to a mixed saturation of mechanical degraded polymers from the higher rate injections. It may result in a lower resistant factor at low injection rates where a high rate was recently injected.

The degree of shear thickening in HPAM 3630S seems to be larger in the porous media, however we know that the geometry in the rheometer have limitations that makes the rest of the shear thickening region unknown. If there is a larger degree of shear thickening in the porous media, this could be contributed to the effect of small relaxation time compared to transit time in the pores. HPAM 3230S in-situ seems to have better matching viscosity curves compared to the rheometer results. It may be because the degree of viscoelasticity makes for differences in rheological behavior in-situ and in the rheometer.

All of the polymer concentrations show a shear thinning region in porous media at the lower part of the apparent shear rates. Previous work [20] shows that this shear thinning behavior only occurs in short segments of porous media. The larger polymer component that causes this behavior propagates slowly and will not penetrate deep into a porous media. [20]

The apparent viscosity in the cores is also lower than the rheometer viscosity; this could be contributed to two factors. The slip phenomenon effect (polymer adhesion to pore walls) makes the polymer slide easier through the pores, and thus lowering the viscous force. [17]

The other factor may be that the permeability is higher during the injection than what is measured afterwards, resulting in false apparent viscosity calculations.

The mechanical degradation of the polymer solutions can be seen through the effluent rheometer measurements. HPAM 3630S 800ppm show evident signs of degradation at both low and high injection rates with the most significant degradation at high injection rate. However, it is surprising to see that the effluent samples of 3630S 2000ppm show very similar rheological behavior for both high and low injection rates.

HPAM 3230S for both concentrations show little or no signs of mechanical degradation at low injection rates. At effluent samples during high injection rate, a rather small reduction in viscosity is observed at medium to low shear rates. The degradation at high injection rate seems to only affect the viscous properties at lower shear rates.

The rheology comparison in porous media between the equivalent concentrations of 3630S and 3230S show that HPAM 3230S generally have a higher resistant factor at medium to low injection rates. The viscoelastic effect seems to occur earlier for HPAM 3630S, yielding in a higher resistant factor at high rates. This can also be seen in the rheometer measurements. The magnitude and length of the shear thickening region can unfortunately not be seen due to range restrictions in the differential pressure gauges.

4.6 Summary

Summary of results and discussion:

- HPAM 3230S shows less viscous properties per ppm than HPAM 3630S
- HPAM 3230S shows smoother viscosity curves, a later onset of shear thickening and a less steep shear thinning region
- No signs of deviations in core HF 2 and HF B when it comes to whether the injection rate starts descending or rising
- Permeability differences after the rate is descending and increasing seem to make the resistant factor higher at higher injection rates for 800ppm 3630S
- The resistant factor at medium to low injection rates for 3630S 800ppm and 3230S 1500ppm seems to be higher when the injection rate starts at the minimum injection rate. This might be due to a mixed saturation of mechanical degradation from the higher rate injections.
- The degree of shear thickening in HPAM 3630S seems to be larger in porous media for both polymers although limitations in the rheometer geometry leaves end of curve unknown
- HPAM 3230S in porous media seems to have a better match of viscosity curves compared to rheometer measurements
- All the polymer viscosity curves in porous media show a shear thinning region before shear thickening. This is believed to be an effect only seen in short segments of porous media. [20]
- Apparent viscosities are lower than the rheometer measurements. This could be attributed to a slip effect [17] and false permeability assumptions
- 800ppm 3630S shows evident signs of mechanical degradation I porous media with the most significant degradation at high injection rates
- 2000ppm 3630S shows mechanical degradations, but surprisingly the level of degradation seems similar for high and low rate injections

- HPAM 3230S shows little or no signs of degradation at low injection rates and degradation at high rates is a lot smaller compared to HPAM 3630S and only occurs as lower injection rates
- Comparison of equivalent concentrations of HPAM 3630S and 3230S in porous media shows that 3230S have a higher resistant factor at medium to low injection rates
- The viscoelastic effect seems to occur earlier for HPAM 3630S both in porous media and in the rheometer, yielding in a higher resistant factor at higher injection rates
- Permeability seems to decrease more after injection of HPAM 3630S than injection of 3230S

5 Conclusion

Viscosity is defined by the premises of a Newtonian fluid.

The effective (shear) viscosity for a non-Newtonian fluid is defined as the equivalent Newtonian viscosity that results in the same shear stress at a surface at equal volumetric flow rates. Apparent viscosities for polymers in porous media can be calculated by using Darcy's law. The apparent shear rates in the porous media are proportional to the injection rate. The shear rate can be related to permeability, porosity and a pore geometry constant by using the shear rate for Newtonian fluids in a capillary tube.

The viscosity and thus injectivity of polymers in porous media gives us important information because it yields information about the polymers mobility (sweep efficiency) and viscous force (limitations in injection equipment).

In the experiments it was found that the rheological behavior of viscoelastic synthetic polymers is different from rheometer measurements. The degree of shear thickening (viscoelasticity) seems to be larger in porous media, a steeper viscosity increase compared to what was expected, especially for the high molecular weight polymer. In the rather short cores used for injections there was also an evident shear thinning region at injection rates lower than the onset of shear thickening.

In the rheometer data there was found to be a large deviation in viscous properties for high molecular weight and low molecular weight polymers. The low molecular polymer did not only show less viscosity per ppm solution, but also a less shear thinning and shear thickening effect at concentrations where the viscosity was nearly identical at shear rate $10s^{-1}$.

The viscous behavior in porous media showed that the low molecular weight polymer showed a later onset of shear thickening, although more viscous at medium to low injection rates than what to be expected from rheometer results.

Low molecular weight synthetic polymers could be an alternative to high molecular weight synthetic polymers if less viscoelastic properties yet high resistant factor at lower injection rates are desired.

The low molecular weight polymer also seems to be a choice of preference if less permeability reduction or less mechanical degradation is wanted. Keep in mind that low synthetic polymer solutions requires a higher concentration of polymer molecules to reach sufficient viscous properties overall.

6 Further Work

Possible further work concerning the subjects and experimental work presented in this thesis:

- Longer core, bigger cores or more cores

- Better or different range of the differential pressure gauges

- Different types of polymers and concentrations (bio- and synthetic)

- Higher pressures (injection rates)

- Different types of rock

- Radial flow through discs

- Rheology of polymers injected into cores saturated with oil

- Injection of other non-Newtonian fluids

- Use core samples with different wettabilities

- Investigate the effect of different pore size distributions

- Three phases present in the porous media

- Polymers wettability properties

- Microscopic scale behavior

- Annular gap rheometer

- Effect of temperature

- Oscillating rheometer measurements

- Polymer rheology when combined with surfactants

References

[1]   Energy4me,   Petroleum   –   Oil   and   Natural Gas Available:[http://www.energy4me.org/energy-facts/energy-sources/petroleum/] [Retrieved: 28.04.2014].

[2] Lien J R, Jacobsen M, Skauge A (2007), *PTEK100 Introduksjon til petroleums- og prosessteknologi*, Compendium, University of Bergen

[3] Norwegian Petroleum Directorate (2011), *Opportunities and challenges for producing field,* Available:[http://www.npd.no/en/Publications/Resource-Reports/2011/Chapter-5/] [Retrieved: 28.04.2014]

[4] Zolotuchin AB, Ursin J-R (2000), *Introduction to Petroleum Reservoir Engineering,* Kristiansand: Høyskoleforl. VIII, 407 s. p.

[5] Ahmed T (2006), *Reservoir Engineering Handbook*, Amsterdam: Elsevier. XV, 1360 s. p.

[6] Lien JR (2010), *PTEK212 Reservoarteknikk 1*, Compendium, University of Bergen

[7] Azom.com, *How does Temperature Change Viscosity in Liquids and Gases?* Available:[http://www.azom.com/article.aspx?ArticleID=10036] [Retrieved: 30.04.2014]

[8] Schramm G (2000), *A Practical Approach to Rheology and Rheometry*, Karlsruhe, Germany, Thermo Haake, 291 s.p.

[9] Bear J (1972), *Dynamics of Fluid in Porous Media*, New York, American Elsevier, 764 s.p.

[10] Skarestad M, Skauge A (2012), *PTEK213 Reservoarteknikk II*, Compendium, University of Bergen

[11] Sadowski T J, Bird R B (1965) Trans. Soc. Rheol. 9 No. 2, 243

[12] Cengel Y A, Cimbala J M (2010), *Fluid Mechanics Fundamentals and Applications*, New York, McGraw-Hill Education, 980 s.p.

[13] Taha Sochi (2009), *Single-Phase Flow of Non-Newtonian Fluids in Porous Media*, University College London, Department of Physics and Astronomy

[14] Corapcioglu M Y (1996), *Advances in Porous Media, New York, Elsevier*, 439 s.p.

[15] Phan-Thien N (2002), *Understanding Viscoelasticity*, National University of Singapore, Springer, 143 s.p.

[17] Sorbie KS (1991), *Polymer-improved oil recovery*, Glasgow: Blackie. xii, 359 s. : ill. p.

[18] Bird R B, Stewart W E, Lightfoot E N (1960), *Transport Phenomena*, New York, Wiley

[19] Savins J G (1969), Ind. Eng. Chem. 61, 18

[20] Seright R S, Fan T, Wavrik K (2010), *New Insights into Polymer Rheology in Porous Media*, SPE Journal 16, 35-42

Appendix

A. HPAM 3630S Rheometer Results

Table 5: Rheometer results for HPAM 3630S up to 800ppm.

Shear rate [s⁻¹]	100ppm: Shear viscosity [cP]	200ppm: Shear viscosity [cP]	400ppm: Shear viscosity [cP]	600ppm: Shear viscosity [cP]	800ppm: Shear viscosity [cP]
0,01					
0,01585					
0,02512					
0,03981					
0,0631					
0,1					
0,1585					
0,2512					
0,3981					32,2
0,631					31,51
1					30,17
1			6,471	15,41	30,46
1,259			6,751	15,75	29,28
1,585			6,764	15,37	27,83
1,995		2,689	6,942	14,71	26,16
2,512		2,703	6,924	14,45	24,6
3,163		2,806	6,888	13,75	23,09
3,981		2,862	6,832	13,04	21,53
5,012		2,882	6,697	12,47	20,09
6,31		2,813	6,391	11,67	18,63
7,944	1,529	2,825	6,185	11,03	17,3
10	1,555	2,764	5,949	10,38	16,02
10	1,56	2,78	5,96	10,39	16,06
12,59	1,558	2,712	5,698	9,742	14,86
15,85	1,56	2,648	5,452	9,139	13,75
19,95	1,558	2,605	5,197	8,546	12,74
25,12	1,543	2,542	4,952	8,019	11,84
31,62	1,564	2,494	4,73	7,562	11,07
39,81	1,564	2,433	4,5	7,138	10,46
50,12	1,592	2,453	4,35	6,844	9,803
63,1	1,688	2,531	4,236	6,501	9,255
79,44	1,937	3,259	5,816	7,014	11,05
100	2,322	3,579	6,079	8,478	11,64
125,9	2,631	3,811	6,191	9,126	12,16
158,5	2,904	4,005	6,343	9,381	13,16
199,5	3,156	4,307	6,571	10,45	13,78
251,2	3,43	4,869	7,462	11,57	15,84
316,2	3,76	5,261	8,165	12,55	17,91
398,1	4,191	5,796	9,618	14,89	21,68
501,2	4,697	6,601	10,31	18,96	
631	5,24	7,124	12,08		
794,4	5,822	7,645	14,31		
1000	6,423	8,238			
1000	6,401	8,017			
2000	10,04	9,701			
3000					
4000					
5000					

Table 6: Rheometer results for HPAM 3630S over 800ppm.

Shear rate [s⁻¹]	1000ppm: Shear viscosity [cP]	1500ppm: Shear viscosity [cP]	2000ppm: Shear viscosity [cP]	3000ppm: Shear viscosity [cP]	5000ppm: Shear viscosity [cP]
0,01				3242	
0,01585			876,8	3192	
0,02512			856,4	2863	
0,03981			809,1	2444	
0,0631		203,7	713,5	2009	
0,1		196,5	593,7	1609	6797
0,1585	55,07	186,4	476,9	1279	5043
0,2512	57,18	172,5	388,9	1010	3743
0,3981	51,77	151,8	322,7	784,2	2753
0,631	50,47	129,6	264,5	601,1	2015
1	46,23	109,2	208,1	456,7	1478
1	45,53	108,6	212,1	460	
1,259	43,27	99,05	187	398,7	
1,585	39,89	89,46	169,4	347,4	1092
1,995	37,05	81,25	148,6	302,3	
2,512	34,57	73,22	132,1	263,4	810,6
3,163	31,63	66,06	117,8	229,5	
3,981	29,2	59,21	104,1	200,7	596,2
5,012	26,73	53,21	92,42	175,5	
6,31	24,63	47,85	82,5	153,6	434,7
7,944	22,57	43	73,28	134,2	
10	20,67	38,79	65,13	117,2	317,4
10	20,68	38,93	65,24	117,1	
12,59	18,94	35,14	58,08	102,2	
15,85	17,38	31,81	51,82	89,63	232,6
19,95	16,04	28,85	46,38	78,76	
25,12	14,92	26,22	41,66	69,38	171,5
31,62	13,81	23,85	37,55	61,3	
39,81	12,75	21,76	34,06	54,25	127,5
50,12	11,81	19,94	31,51	48,15	
63,1	11,01	18,37	29,69	42,84	95,45
79,44	10,37	17,3	33,01	38,21	
100	13,65	20,88	29,88	34,15	84,23
125,9	13,69	20,19	29,34	40,92	
158,5	14,55	20,31	30,59	44,18	
199,5	15,59	22,81	37,28	62,88	
251,2	17,86	29,61	46,6		
316,2	23,4	37,39			
398,1	30,91				
501,2					
631					
794,4					
1000					
1000					
2000					
3000					
4000					
5000					

B. HPAM 3230S Rheometer Results

Table 7: Rheometer results for HPAM 3230S up to 800ppm.

Shear rate [s⁻¹]	100ppm: Shear viscosity [cP]	200ppm: Shear viscosity [cP]	400ppm: Shear viscosity [cP]	600ppm: Shear viscosity [cP]	800ppm: Shear viscosity [cP]
0,01					
0,01585					
0,02512					
0,03981					
0,0631					
0,1					
0,1585					
0,2512					
0,3981					
0,631					9,953
1					9,552
1	1,514			5,684	9,973
1,259	1,527	1,905	3,681	5,753	9,728
1,585	1,52	1,91	3,589	5,611	9,398
1,995	1,497	1,786	3,332	5,551	9,157
2,512	1,357	1,836	3,278	5,415	9,083
3,163	1,348	1,801	3,265	5,394	9,036
3,981	1,439	1,877	3,404	5,488	8,731
5,012	1,37	1,817	3,351	5,436	8,793
6,31	1,268	1,763	3,235	5,297	8,448
7,944	1,306	1,826	3,282	5,27	8,205
10	1,303	1,806	3,23	5,17	7,986
10	1,306	1,831	3,234	5,19	7,997
12,59	1,314	1,819	3,195	5,065	7,763
15,85	1,291	1,791	3,157	4,966	7,53
19,95	1,271	1,775	3,102	4,855	7,273
25,12	1,263	1,76	3,028	4,704	6,263
31,62	1,28	1,77	2,981	4,612	6,026
39,81	1,257	1,72	2,901	4,462	5,854
50,12	1,269	1,728	2,849	4,365	5,622
63,1	1,267	1,721	2,753	4,203	5,444
79,44	1,337	1,811	2,79	4,142	5,271
100	1,429	1,725	2,687	3,992	4,994
125,9	1,441	1,785	2,684	3,873	4,843
158,5	1,569	1,895	2,721	3,831	4,679
199,5	1,773	2,097	2,87	3,864	4,654
251,2	2,021	2,323	3,012	4,025	4,692
316,2	2,224	2,553	3,229	4,218	4,744
398,1	2,495	2,854	3,529	4,462	4,86
501,2	2,778	3,189	3,895	4,797	5,168
631	3,146	3,546	4,335	5,206	5,542
794,4	3,595	4,021	4,849	5,731	6,016
1000	4,164	4,601	5,464	6,353	6,645
1000			5,461	6,352	6,631
2000			9,666	10,23	10,71
3000					
4000					
5000					

Table 8: Rheometer results for HPAM 3230S over 800ppm.

Shear rate [s⁻¹]	1000ppm: Shear viscosity [cP]	1500ppm: Shear viscosity [cP]	2000ppm: Shear viscosity [cP]	3000ppm: Shear viscosity [cP]	5000ppm: Shear viscosity [cP]
0,01					
0,01585					
0,02512					
0,03981					
0,0631					
0,1		31,46		116,1	606,6
0,1585		30,61	45,29	112	569,3
0,2512		27,66	46,42	112,2	541,3
0,3981		23,34	46,81	112,1	501,6
0,631		24,22	44,18	108,7	462,4
1		22,27	44,26	104,5	419,2
1	11,76	22,89	43,28	103,9	
1,259	11,56	22,34	43,47	102,2	
1,585	11,53	22,18	42,63	98,63	371
1,995	10,82	21,3	42,41	95,16	
2,512	11,19	21,42	41,14	91,63	320,6
3,163	11,01	20,9	40,03	88,01	
3,981	10,64	20,25	39,08	83,53	271
5,012	10,68	19,9	37,58	79,17	
6,31	10,37	19,25	36,24	74,45	224,6
7,944	10,22	18,71	34,58	69,8	
10	9,966	18,04	32,9	65,11	182,8
10	9,949	18,04	32,91	65,14	
12,59	9,672	17,34	31,19	60,45	
15,85	9,425	16,61	29,43	55,9	146,6
19,95	9,079	15,85	27,65	51,47	
25,12	8,76	15,09	25,85	47,25	116,3
31,62	8,43	14,28	24,11	43,2	
39,81	8,029	13,46	22,3	39,39	91,73
50,12	7,676	12,68	20,66	35,83	
63,1	7,354	11,89	19,07	32,51	72,46
79,44	7	11,16	17,58	29,52	
100	6,683	10,45	16,2	26,79	57,38
125,9	6,369	9,792	14,98	24,39	
158,5	6,09	9,17	13,83	22,06	
199,5	5,896	8,651	12,81	20,17	
251,2	5,791	8,208	12,01	18,44	
316,2	5,783	7,942	11,23	16,91	
398,1	5,872	7,791	10,76	15,77	
501,2	6,02	7,799	10,33	14,86	
631	6,334	7,894	10,13	14,19	
794,4	6,742	8,252	10,82	15,14	
1000	7,382	8,972	11,47	14,96	
1000	7,368	8,995	11,49	14,95	
2000	11,72	13,76	14,09	19,1	
3000			18,89		
4000					
5000					

C. Core and Injection Data HPAM 3630S

Table 9: Core data for HPAM 3630S injections.

Differential Pressure Gauge	**dP2**	**dP1**
Bentheimer Sandstone	**Core HF 2**	**Core HF 1**
Diameter [cm]:	3.76	3.74
Length [cm]:	5.84	5.63
Cross-sectional Area [cm^2]	11.10	10.99
Pore Volume [mL]:	14.8	15.2
Porosity	0.24	0.26
Permeability Before Polymer Injection [mD]	1734	1963
Pore Geometry Constant α (picked)	5	3

Table 10: Injection data and calculations for HPAM 3630S 800ppm high to low injection rate.

Q [mL/min]	dP2 [mBar]	dP1 [mBar]	RF2 (HF 2) [cP]	RF (HF1) [cP]	Shear rate (HF 2) [s^{-1}]	Shear rate (HF 1) [s^{-1}]
4	4751		46		1044,7	936,9
3,5	3821		42		914,1	819,8
3	2911		37		783,6	702,7
2,5	2076		32		653,0	585,6
2	1346	1110	26	10	522,4	468,5
1,5	791	655	20	8	391,8	351,4
1	354,3	315,8	13,7	5,6	261,2	234,2
0,7	177,3	170,8	9,8	4,3	182,8	164,0
0,3	36,8	50,3	4,7	3,0	78,4	70,3
0,1	10,8	20,8	4,1	3,7	26,1	23,4
0,08	8,5	17,0	4,1	3,8	20,9	18,7
0,03	3,6	8,4	4,6	5,0	7,8	7,0

Table 11: Absolute permeability after HPAM 3630S 800ppm high to low injection rate.

Core	HF 2	HF 1
Permeability [mD]	**332**	**157**

Table 12: Injection data and calculations for HPAM 3630S 800ppm low to high injection rate.

Q [mL/min]	dP2 [mBar]	dP1 [mBar]	RF2 (HF 2) [cP]	RF (HF1) [cP]	Shear rate (HF 2) [s⁻¹]	Shear rate (HF 1) [s⁻¹]
0,08	8,3	27,6	4,1	5,0	20,8	20,6
0,1	9,8	32,3	3,8	4,7	26,0	25,8
0,3	35,3	72,3	4,6	3,5	78,0	77,3
0,7	171,3	201,8	9,6	4,2	182,1	180,5
1	340,8	343,8	13,4	5,0	260,1	257,8
1,5	753	690	20	7	390,1	386,7
2	1326	1140	26	8	520,2	515,6
2,5	2051		32		650,2	644,5
3	2891		38		780,3	773,4
3,5	3756		42		910,3	902,3
4	4651		46		1040,3	1031,2

Table 13: Absolute permeability after HPAM 3630S 800ppm low to high injection rate.

Core	HF 2	HF 1
Permeability [mD]	**335**	**129**

Table 14: Injection data and calculations for HPAM 3630S 2000ppm high to low injection rate.

Q [mL/min]	dP2 [mBar]	dP1 [mBar]	RF2 (HF 2) [cP]	RF (HF1) [cP]	Shear rate (HF 2) [s⁻¹]	Shear rate (HF 1) [s⁻¹]
3					942,0	777,1
2,5	4401		47		785,0	647,6
2	2801		38		628,0	518,1
1,5	1611	1340	29	13	471,0	388,5
1	746	660	20	10	314,0	259,0
0,7	391,3	384,8	15,1	7,9	219,8	181,3
0,3	98,3	169,8	8,8	8,2	94,2	77,7
0,1	34,3	67,8	9,2	9,8	31,4	25,9
0,07	26,3	53,8	10,1	11,1	22,0	18,1
0,03	16,3	35,8	14,6	17,2	9,4	7,8
0,01	6,8	19,3	18,2	27,9	3,1	2,6

Table 15: Absolute permeability after HPAM 3630S 2000ppm high to low injection rate.

Core	HF 2	HF 1
Permeability [mD]	**230**	**128**

Table 16: Injection data and calculations for HPAM 3630S 2000ppm low to high injection rate.

Q [mL/min]	dP2 [mBar]	dP1 [mBar]	RF2 (HF 2) [cP]	RF (HF1) [cP]	Shear rate (HF 2) [s^{-1}]	Shear rate (HF 1) [s^{-1}]
0,01	11,3	20,6	31,2	31,2	3,1	2,5
0,03	18,8	33,3	17,3	16,8	9,3	7,6
0,07	25,3	63,8	10,0	13,8	21,6	17,8
0,1	33,3	78,3	9,2	11,8	30,9	25,4
0,3	93,8	133,8	8,7	6,7	92,6	76,3
0,7	376,3	359,8	14,9	7,8	216,1	178,0
1	721	635	20	10	308,7	254,3
1,5	1526	1275	28	13	463,0	381,5
2	2701		37		617,3	508,6
2,5	4001		44		771,7	635,8

Table 17: Absolute permeability after HPAM 3630S 2000ppm low to high injection rate.

Core	HF 2	HF 1
Permeability [mD]	**238**	**133**

D. Core and Injection Data HPAM 3230S

Table 18: Core data for HPAM 3230S injections.

Differential Pressure Gauge	dP2	dP1
Bentheimer Sandstone	**Core HF B**	**Core HF A**
Diameter [cm]:	3.77	3.76
Length [cm]:	5.57	5.55
Cross-Sectional Area [cm^2]	11.16	11.10
Porevolume [mL]:	14.9	15.2
Porosity	0.24	0.25
Permeability Before Polymer Injection [mD]	1373	1922
Pore Geometry Constant α (picked)	5	5

Table 19: Injection data and calculations for HPAM 3230S 1500ppm high to low injection rate.

Q [mL/min]	dP2 [mBar]	dP1 [mBar]	RF2 (HF B) [cP]	RF (HF A) [cP]	Shear rate (HF B) [s^{-1}]	Shear rate (HF A) [s^{-1}]
10	1901	1155	17	10	1780,5	1759,3
7	1081	640	14	8	1246,4	1231,5
3	306,3	199,8	9,0	5,9	534,2	527,8
1	89,3	67,8	7,8	6,0	178,1	175,9
0,7	63,8	50,3	8,0	6,4	124,6	123,1
0,3	29,8	25,3	8,7	7,5	53,4	52,8
0,1	11,4	10,0	10,0	8,9	17,8	17,6
0,07	8,3	7,4	10,4	9,3	12,5	12,3
0,03	3,8	3,4	11,1	10,1	5,3	5,3
0,01	1,3	1,4	11,0	12,5	1,8	1,8

Table 20: Absolute permeability after HPAM 3230S 1500ppm high to low injection rate.

Core	HF B	HF A
Permeability [mD]	**740**	**750**

Table 21: Injection data and calculations for HPAM 3230S 1500ppm low to high injection rate.

Q [mL/min]	dP2 [mBar]	dP1 [mBar]	RF2 (HF B) [cP]	RF (HF A) [cP]	Shear rate (HF B) [s^{-1}]	Shear rate (HF A) [s^{-1}]
0,01	1,3	1,5	11,2	14,1	1,8	1,7
0,03	3,5	4,3	10,5	13,5	5,3	5,1
0,07	7,8	8,7	10,0	11,6	12,3	12,0
0,1	10,9	11,7	9,7	10,9	17,6	17,1
0,3	29,1	27,9	8,7	8,7	52,9	51,4
0,7	62,8	55,8	8,0	7,5	123,4	119,9
1	88,3	75,8	7,9	7,1	176,2	171,3
3	291,3	212,8	8,7	6,7	528,7	513,9
7	1021	645	13	9	1233,5	1199,1
10	1761	1110	16	10	1762,2	1712,9

Table 22: Absolute permeability after HPAM 3230S 1500ppm low to high injection rate.

Core	HF B	HF A
Permeability [mD]	**755**	**791**

Table 23: Injection data and calculations for HPAM 3230S 3000ppm high to low injection rate.

Q [mL/min]	dP2 [mBar]	dP1 [mBar]	RF2 (HF B) [cP]	RF (HF A) [cP]	Shear rate (HF B) [s^{-1}]	Shear rate (HF A) [s^{-1}]
10	3641		26		1968,4	2115,2
7	2131	1360	22	12	1377,9	1480,6
3	646	445	15	9	590,5	634,6
1	219,3	176,8	15,8	11,1	196,8	211,5
0,7	164,3	148,8	16,9	13,3	137,8	148,1
0,3	87,8	84,3	21,0	17,6	59,1	63,5
0,1	38,6	39,8	27,7	25,0	19,7	21,2
0,07	29,3	31,1	30,0	27,9	13,8	14,8
0,03	14,5	18,1	34,6	37,8	5,9	6,3
0,01	10,2	4,2	73,0	26,3	2,0	2,1

Table 24: Absolute permeability after HPAM 3230S 3000ppm high to low injection rate.

Core	HF B	HF A
Permeability [mD]	**605**	**519**

Table 25: Injection data and calculations for HPAM 3230S 3000ppm low to high injection rate.

Q [mL/min]	dP2 [mBar]	dP1 [mBar]	RF2 (HF B) [cP]	RF (HF A) [cP]	Shear rate (HF B) [s^{-1}]	Shear rate (HF A) [s^{-1}]
0,01	5,8	6,6	36,6	34,8	2,1	2,3
0,03	14,8	15,9	31,0	28,1	6,3	6,8
0,07	30,8	39,3	27,7	29,8	14,7	15,9
0,1	43,3	58,8	27,3	31,2	21,0	22,8
0,3	99,3	119,8	20,9	21,2	63,0	68,3
0,7	187,3	203,8	16,9	15,5	147,1	159,4
1	248,3	257,8	15,7	13,7	210,1	227,7
3	681	550	14	10	630,4	683,2
7	2171		20		1470,9	1594,2
10	3631		23		2101,2	2277,5

Table 26: Absolute permeability after HPAM 3230S 3000ppm low to high injection rate.

Core	HF B	HF A
Permeability [mD]	**531**	**448**

E. Effluent HPAM 3630S Rheometer Results

Table 27: Effluent rheometer results for HPAM 3630S.

Shear rate [s⁻¹]	800ppm 0.03mL/min Shear viscosity [cP]	800ppm 3mL/min Shear viscosity [cP]	2000ppm 0.01mL/min Shear viscosity [cP]	2000ppm 2mL/min Shear viscosity [cP]
0,01				
0,01585				
0,02512				
0,03981				
0,0631				
0,1				
0,1585				
0,2512			86,75	69
0,3981			83,05	67
0,631			79,27	67,08
1			71,72	63,34
1	22,16		70,77	62,42
1,259	21,8		67,78	60,33
1,585	21,28		63,67	56,84
1,995	20,18		59,16	53,7
2,512	19,28		54,87	50,7
3,162	18,13	8,514	50,69	47,33
3,981	17,19	8,521	46,81	44,09
5,012	16	8,537	43,16	41,01
6,31	15,05	8,327	39,27	37,81
7,944	14,07	8,188	35,77	34,76
10	13,13	7,984	32,57	31,88
10	13,12	8,002	32,57	31,91
12,59	12,2	7,753	29,6	29,2
15,85	11,33	7,493	26,88	26,66
19,95	10,52	7,228	24,41	24,31
25,12	9,76	6,919	22,19	22,14
31,62	9,11	6,635	20,27	20,15
39,81	8,532	6,3	18,53	18,39
50,12	8,064	6,051	16,99	16,82
63,1	7,65	5,773	15,6	15,51
79,44	7,292	5,469	14,4	14,24
100	6,99	5,184	13,58	13,12
125,9	9,016	5,003	13,27	12,03
158,5	9,313	4,876	14,72	11,16
199,5	9,225	4,846	14	10,53
251,2	9,508	5,038	14,4	12,91
316,2	10,72	5,585	14,69	12,7
398,1	13,11	5,879	16,86	12,42
501,2	15,62	6,323	18,4	13,01
631	19,48	6,842	20,68	13,58
794,4		7,411	21,86	14,63
1000		8,236	22,14	17,08
1000		8,26	21,74	16,93
2000		13,42	22,58	21,79
3000			25,88	25,26
4000				
5000				

F. Effluent HPAM 3230S Rheometer Results

Table 28: Effluent rheometer results for HPAM 3230S.

Shear rate [s⁻¹]	1500ppm 0.03mL/min Shear viscosity [cP]	1500ppm 3mL/min Shear viscosity [cP]	3000ppm 0.01mL/min Shear viscosity [cP]	3000ppm 2mL/min Shear viscosity [cP]
0,01				
0,01585				
0,02512				
0,03981				
0,0631				
0,1			108,5	
0,1585			108,7	
0,2512			108,1	91,24
0,3981			111,3	87,66
0,631			106,4	89,08
1			102,7	88,09
1	22,06	16,89	101,4	87,46
1,259	21,43	16,68	99,18	86,3
1,585	21,42	16,27	96,73	84,75
1,995	21,38	16,31	93,47	83,33
2,512	20,99	16,45	89,82	81,27
3,162	20,64	16,07	85,64	79,03
3,981	20,32	15,95	81,65	76,12
5,012	19,72	15,97	77,24	73,08
6,31	19,33	15,53	72,83	69,63
7,944	18,74	15,29	68,24	66,08
10	18,1	15,01	63,68	62,32
10	18,12	14,99	63,78	62,38
12,59	17,45	14,65	59,31	58,47
15,85	16,72	14,25	54,84	54,53
19,95	15,97	13,8	50,52	50,62
25,12	15,19	13,3	46,38	46,78
31,62	14,41	12,74	42,46	43,04
39,81	13,61	12,2	38,77	39,48
50,12	12,82	11,59	35,28	36,06
63,1	12,07	11,04	32,06	32,92
79,44	11,38	10,56	29,07	30,01
100	10,62	9,826	26,36	27,18
125,9	9,916	9,255	23,89	24,59
158,5	9,297	8,702	21,72	22,26
199,5	8,752	8,221	19,85	20,15
251,2	8,336	7,814	18,09	18,33
316,2	7,994	7,49	16,58	16,73
398,1	7,84	7,324	15,36	15,47
501,2	7,811	7,318	14,52	14,49
631	7,929	7,447	13,91	13,7
794,4	8,811	7,746	14,89	13,36
1000	9,236	8,266	15,14	13,32
1000	9,232	8,261	15,14	13,32
2000	11,47	12,06	18,32	16,77
3000	15,42			
4000				
5000				